

Current status of turbulent dynamo theory

From large-scale to small-scale dynamos

Axel Brandenburg, Dmitry Sokoloff,
Kandaswamy Subramanian

March 11, 2021, Revision: 1.138

Abstract Several recent advances in turbulent dynamo theory are reviewed. High resolution simulations of small-scale and large-scale dynamo action in periodic domains are compared with each other and contrasted with similar results at low magnetic Prandtl numbers. It is argued that all the different cases show similarities at intermediate length scales. On the other hand, in the presence of helicity of the turbulence, power develops on large scales, which is not present in non-helical small-scale turbulent dynamos. At small length scales, differences occur in connection with the dissipation cutoff scales associated with the respective value of the magnetic Prandtl number. These differences are found to be independent of whether or not there is large-scale dynamo action. However, large-scale dynamos in homogeneous systems are shown to suffer from resistive slow-down even at intermediate length scales. The results from simulations are connected to mean field theory and its applications. Recent work on helicity fluxes to alleviate large-scale dynamo quenching, shear dynamos, nonlocal effects and magnetic structures from strong density stratification are highlighted. Several insights which arise from analytic considerations of small-scale dynamos are discussed.

Keywords magnetic fields · turbulence · Sun: magnetic fields

PACS 44.25.+f · 47.27.Eq · 47.27.Gs · 47.27.Qb

A. Brandenburg
Nordita, Royal Institute of Technology and Stockholm University, Roslagstullsbacken 23,
10691 Stockholm, Sweden; and Department of Astronomy, Stockholm University, SE 10691
Stockholm, Sweden, E-mail: brandenb@nordita.org

D. Sokoloff
Department of Physics, Moscow University, 119992 Moscow, Russia, E-mail:
d.sokoloff@hotmail.com

K. Subramanian
Inter-University Centre for Astronomy and Astrophysics, Post Bag 4, Ganeshkhind, Pune 411
007, India, E-mail: kandu@iucaa.ernet.in

1 Introduction

Dynamos convert kinetic energy into magnetic energy. In the astrophysical context, one always means by a dynamo a self-excited device, except that the conductivity is uniformly distributed and not limited to conducting wires in an insulating container, as in laboratory dynamos. Since the beginning of the space age, it is well understood that such a device can work, at least in principle. The discovery of the first rigorously proven example by Herzenberg (1958) was significant, even though the particular configuration studied by him was not of immediate astrophysical interest. The Herzenberg configuration consists of a uniformly conducting solid medium (e.g., copper) with two or more conducting rotors in electrical contact with the rest. Dynamo action is possible when the rotors spin faster than a certain critical value that depends on the angle between the rotors. For angles between 90 and 180 degrees the solutions are non-oscillatory, while for angles between 0 and 90 degrees there are oscillatory solutions that were discovered only more recently (Brandenburg et al. 1998).

The Herzenberg dynamo belongs to the class of “slow” dynamos, for which the dynamo growth rate is maximum for intermediate values of the conductivity, but it returns to zero in the limit of perfect conductivity. Another example of a slow dynamo is the Roberts flow, which consists of a steady two-dimensional flow pattern, $\mathbf{u} = \mathbf{u}(x, y)$, but all three flow components are non-vanishing. This dynamo was first studied by Roberts (1970, 1972). It provides an important benchmark of a large-scale dynamo, where magnetic field on scales larger than the scale of motions are produced, by a mechanism called the α effect. Here, α refers to the name of the coefficient in the relation between mean magnetic field $\overline{\mathbf{B}}$ and mean electromotive force $\overline{\boldsymbol{\mathcal{E}}}$ in a turbulent flow. The basic idea goes back to Parker (1955) who proposed a relation of the form $\overline{\boldsymbol{\mathcal{E}}} = \alpha \overline{\mathbf{B}}$. Later, Steenbeck et al. (1966) computed a tensorial relation of the form $\overline{\mathcal{E}}_i = \alpha_{ij} \overline{B}_j$ for rotating stratified turbulence. It was clear that higher derivatives of the magnetic field would also enter, so a more general expression is

$$\overline{\mathcal{E}}_i = \alpha_{ij} \circ \overline{B}_j + \eta_{ijk} \circ \overline{B}_{j,k}, \quad (1)$$

where the isotropic part of the tensor η_{ijk} , $\eta_{ijk} = \eta_t \epsilon_{ijk}$, corresponds to turbulent magnetic diffusion where η_t is the *turbulent* magnetic diffusivity. The circles indicate convolution over time and space, which is however commonly replaced by a multiplication in the limit in which the integral kernels are well approximated by δ functions in space and time. The work of Steenbeck et al. (1966) marked the beginning of mean-field electrodynamics, which is still the leading theory to explain the amplification of magnetic fields on length scales that are larger than the scale of the energy-carrying turbulent eddies. Such systems are therefore also referred to as large-scale dynamos. Essential here is that the trace of the α tensor is non-vanishing. This typically requires helicity of streamlines (at low conductivity) or of vortex lines (at high conductivity).

In this review we discuss our current knowledge of dynamos covering both large-scale and small-scale turbulent dynamos. In practice, all dynamos of astrophysical relevance tend to be “fast” and thus have a finite growth rate also in the limit of perfect conductivity. There are examples of predetermined flows for which fast dynamo action is indicated by numerical simulations, for example the ABC flow (Galloway and Frisch 1986) and the Galloway and Proctor (1992) flow, but the convergence of the α effect with increasing magnetic Reynolds number can be quite slow or non-existent (see, e.g., Courvoisier et al. 2006). By contrast, when relaxing the assumption of a predetermined kinematic flow pattern and adopting a turbulent flow field, the α effect appears to be

converged for magnetic Reynolds numbers exceeding a critical value of the order of unity up to values of about 200 probed in the simulations (Sur et al. 2008).

We begin by discussing examples of numerical realizations of turbulent dynamos and then turn to some astrophysical examples. Large-scale dynamos produce fields that are well characterized by suitable averages. A theory for describing the evolution of such averaged fields is mean-field theory that is obtained by averaging the governing equations, most notably the induction equation. Large-scale dynamos can then also be referred to as mean-field dynamos (MFD). Under certain conditions, making suitable assumptions about the spatial variation of the α effect, solutions of the mean-field induction equation have been used to characterize the large-scale magnetic fields seen in astrophysical bodies like the Sun and some spiral galaxies. Mean-field theory is also applied to the momentum equation. This leads to a number of effects including turbulent viscosity, the Λ effect (responsible driving differential solar rotation; see Rüdiger 1980, 1989), the anisotropic kinetic alpha effect (Frisch et al. 1987), as well as the negative effective magnetic pressure effect (Kleeorin et al. 1989). In this paper, we also discuss important effects resulting from the mean-field momentum equation, namely the spontaneous formation of magnetic flux concentrations in a strongly stratified layer. Such results may be relevant to explaining the formation of active regions in the Sun.

There is now increased interest in what is known as small-scale or fluctuation dynamos. These are dynamos that can work already under fully isotropic conditions and were anticipated by Batchelor (1950) and others (Biermann and Schlüter 1951; Elsasser 1956), but the now accepted theory was provided by Kazantsev (1967). Fluctuation (or small-scale) dynamos are important in cosmic objects because they are generic to any random flow of a sufficiently conducting plasma. Furthermore, the growth rate is fast and random fields can grow on the eddy turnover timescale of the smallest eddies, which are typically much shorter than the age of the system. This is particularly true of galaxy clusters, for which small-scale dynamos are crucial to explaining the observed magnetic fields, because the conditions for large-scale dynamo action are probably absent (Subramanian et al. 2006).

Small-scale dynamos are nowadays also invoked to describe the small-scale magnetic field at the solar surface. However, in many contexts both small-scale and large-scale dynamos go together. And then it is not clear whether one can (or should) distinguish between a small-scale field from a small-scale dynamo from that associated with the fluctuations that are inherent to any large-scale dynamo and that can be caused by tangling and amplification of the large-scale field.

2 Numerical realizations of turbulent dynamos

Next, we discuss some numerical realizations of turbulent dynamos. By “turbulence” we mean here flows that are solutions to the Navier-Stokes equations that are irregular in space and time, subject to energy injection at large length scales and energy dissipation at short length scales. The ratio between forcing scale to dissipation scale is quantified by the Reynolds number. Throughout this paper, we adopt the following definition for this number:

$$\text{Re} = u_{\text{rms}}/\nu k_{\text{f}}, \quad (2)$$

where $u_{\text{rms}} = \langle \mathbf{u}^2 \rangle^{1/2}$ is the root mean square (rms) value of the turbulent velocity, ν is the kinematic viscosity, and k_{f} is the forcing wavenumber, i.e., the wavenumber

of energy injection. A similar definition is adopted for the *magnetic* Reynolds number, $\text{Re}_M = u_{\text{rms}}/\eta k_f$, where η is the magnetic diffusivity. We also define the magnetic Prandtl number, $\text{Pr}_M = \nu/\eta = \text{Re}_M/\text{Re}$.

At small Reynolds numbers, $\text{Re} \ll 1$, the flow is determined by viscosity and has qualitatively different properties from flows with $\text{Re} \gg 1$. The break point is close to unity, so, for example, a flow with $\text{Re} = 5$ would be called turbulent (or at least mildly turbulent), because it begins to show certain asymptotic scaling properties that are also found for fully turbulent flows. The most famous aspect of fluid turbulence is the Kolmogorov $E_K(k) \sim k^{-5/3}$ energy spectrum, which is normalized such that $\int E_K dk = u_{\text{rms}}^2/2$. Density is omitted in this definition, which requires that density fluctuations are unimportant and the flow is nearly incompressible. In this review we also discuss stratified flows in which density varies strongly due to gravity. In those cases the incompressibility condition $\nabla \cdot \mathbf{u} = 0$ has to be replaced by $\nabla \cdot \rho \mathbf{u} = 0$, which is valid as long as the flows are slow compared with the sound speed and the typical scales of variation smaller than a scale height. However, in the following we do not make such assumptions and consider fully compressible flows.

2.1 Small-scale and large-scale dynamos

We begin by discussing first the difference between small-scale and large-scale dynamos. A small-scale dynamo is one that generates magnetic field at scales much smaller than that of the energy-carrying eddies, while a large-scale dynamo generates field at scales larger than that of the energy-carrying eddies. In many practical situations, the difference is of somewhat academic interest, because the small-scale dynamo is always excited when the magnetic Reynolds number is large, which is the case in many astrophysical situations. Furthermore, the conditions for the excitation of large-scale dynamo action are met in many situations of interest. However, in the case of isotropic turbulence such a distinction can be made by considering helical and non-helical turbulence. In both cases the system can be homogeneous and it makes sense to compute spectra of magnetic and kinetic energy, $E_M(k)$ and $E_K(k)$, respectively; see Figure 1 for $\text{Pr}_M = 1$. The early evolution of such a dynamo is quite similar: both dynamos have a $k^{3/2}$ power spectrum at small scales. Such a scaling was predicted by Kazantsev (1967) (see also Kulsrud and Anderson (1992)) for a single scale non-helical flow which was δ -correlated in time, but seems to be obtained in the simulations more generally. At late times, however, helical turbulence allows the development of an inverse cascade (Frisch et al. 1975) on a longer resistive timescale (see below).

We see that, at least in the saturated state, large-scale dynamos produce and sustain magnetic fields at scales larger than the energy injection scale, while small-scale dynamos produce and sustain magnetic fields at scales smaller than the energy injection scale. The lack of similar behavior in the linear regime could be interpreted as evidence that the underlying mechanism for producing large-scale fields must be nonlinear in nature (Herault et al. 2011). Alternatively, one could interpret the resulting dynamo as a combination of large-scale and small-scale dynamo action, where the latter has a larger growth rate such that in the kinematic regime the field is dominated by the small-scale field, although the large-scale dynamo does still operate in the background. As a consequence it gets the chance to dominate only when the small-scale dynamo has already saturated. Even in this case, and if the Re_M is large, we will argue that

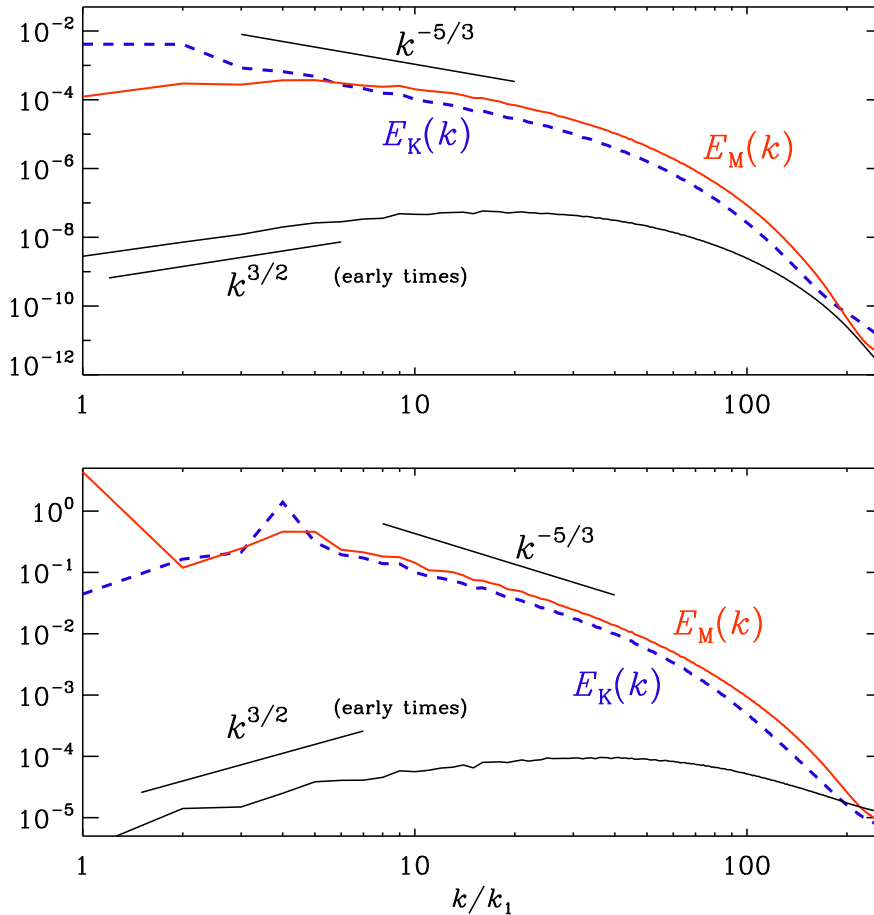


Fig. 1 Kinetic and magnetic energy spectra in a turbulence simulation without net helicity (up) and with net helicity (bottom) for a magnetic Prandtl number of unity and a mesh size is 512^3 meshpoints. Notice the pronounced peak of $E_M(k)$ at $k = k_1$ in the case with helicity. The energy input wavenumbers are $k_f = 1.5k_1$ in the non-helical case (upper panel, $\text{Re}_M = 600$, $\text{Pr}_M = 1$) and $k_f/k_1 = 4$ in the helical case (lower plot, $\text{Re}_M = 450$, $\text{Pr}_M = 1$). Adapted from Brandenburg and Subramanian (2005a) and Brandenburg et al. (2008).

one needs to additionally dissipate small-scale magnetic helicity before the largest scale field can appear.

Both large-scale and small-scale dynamos show that the spectral magnetic energy exceeds the kinetic spectral energy in the beginning of the inertial range. This difference is slightly weaker for large-scale dynamos, but this might be an artifact of the Reynolds number still not being large enough. Such a difference used to be completely absent at Reynolds numbers previously reported; see, for example Brandenburg (2001). The slight super-equipartition was quite evident when simulations at a resolution of 1024^3 meshpoints became first available (Haugen et al. 2003), although this feature can already be seen in earlier simulations (Meneguzzi et al. 1981; Kida et al. 1991). This spectral excess of magnetic fields is expected to diminish as one pro-

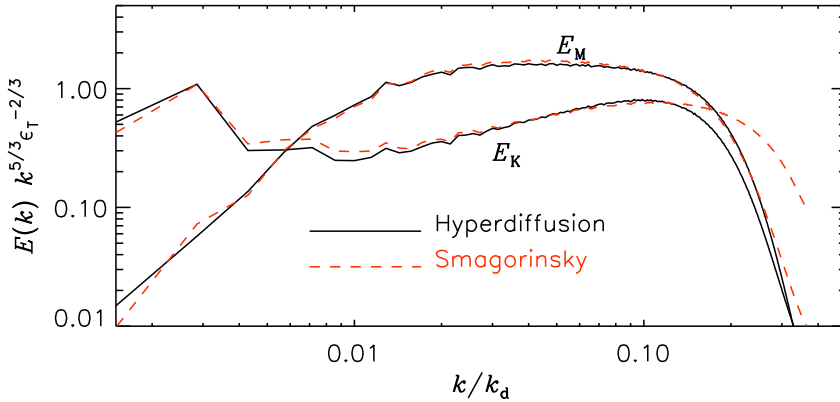


Fig. 2 Magnetic and kinetic energy spectra for runs with 512^3 meshpoints and hyperviscosity with hyperresistivity (solid line) and Smagorinsky viscosity with hyperresistivity (red, dashed line). Note the mutual approach of kinetic and magnetic energy spectra before entering the dissipative subrange. Adapted from Haugen and Brandenburg (2006).

ceeds further down the inertial range. Such behavior was indeed seen in simulations of Haugen and Brandenburg (2006) when using a combination of Smagorinsky viscosity for the velocity field and hyperresistivity for the magnetic field; see Figure 2. This implies that the two spectra cannot be parallel to each other at intermediate length scales, and that the slope of $E_M(k)$ must be slightly steeper than that of $E_K(k)$. This difference in the two slopes at intermediate wavenumbers is now associated with the observed differences in the spectral exponents in the solar wind; see Boldyrev et al. (2011), who find steeper spectra for the magnetic field than the velocity field both from simulations and solar wind observations.

In the spectra of Figure 1 we see a remarkable difference between small-scale and large-scale dynamos. In particular, large-scale dynamos are capable of producing a peak of magnetic energy at the smallest possible wavenumber, while small-scale dynamos do not. On the other hand, we have stated earlier that small-scale and large-scale dynamos are difficult to distinguish in the early stage. In Figure 3 we show the critical values of $Re_M (= Re)$ for dynamo action both for small-scale (non-helical) and large-scale (helical) dynamos. Note that for $Re_M > 35$ the growth rate attains a $Re^{1/2}$ scaling both for small-scale and large-scale dynamos. The same growth rates are also obtained for dynamos driven by convection; see Fig. 15 of Käpylä et al. (2008). This $Re^{1/2}$ scaling of the growth rate of the rms magnetic field, implies that the growth rate is not controlled by the turnover time of the energy-carrying eddies, but of eddies at the dissipation scale (Schekochihin et al. 2002, 2004a). At low values of Re_M , only large-scale dynamo action remains possible. Its excitation condition is determined by the requirement that a certain dynamo number exceeds a critical value. This usually translates to the condition that the degree of scale separation is large enough; see equation (5) of Brandenburg (2009).

An important issue for astrophysical applications is how coherent are the fields generated by small-scale dynamos (Subramanian et al. 2006; Cho and Ryu 2009). On

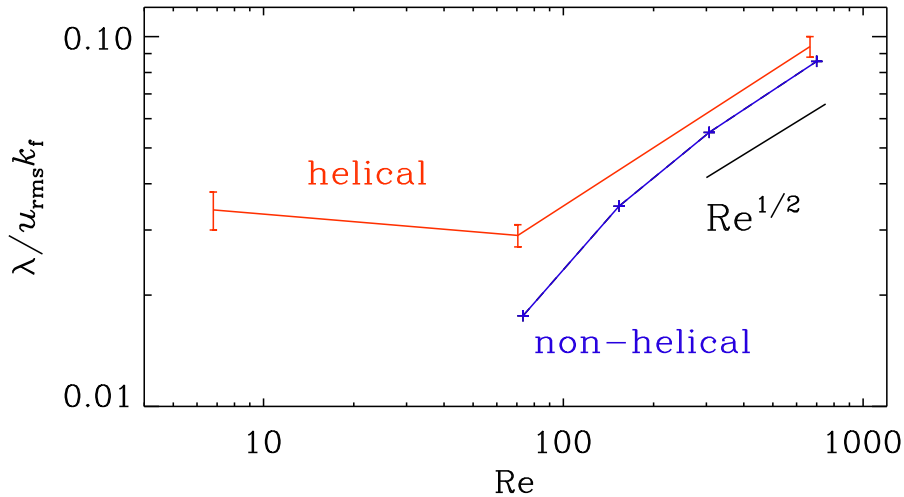


Fig. 3 Dependence of dynamo growth rates of the rms magnetic field on Re_M for helical and non-helical turbulence. Adapted from Brandenburg (2009).

the basis of simulations done with large Pr_M , but small Re , Schekochihin et al. (2004b) argued that the field saturates with a folded structure, where the field reverses at the folds such that power concentrates on resistive scales. The simulations of Haugen et al. (2003, 2004) with $Re_M = Re \gg 1$, found the magnetic correlation lengths $\sim 1/6$ th the velocity correlation length, but much larger than the resistive scale. This seems consistent with the simple Subramanian (1999) model for nonlinear saturation of small-scale dynamos. What happens at large Re and large Pr_M , which is representative of galactic and cluster plasmas, is not easy to capture in simulations. The $Pr_M = 50$, $Re = 80$ simulation described in Brandenburg and Subramanian (2005a), showed evidence for strong field regions with folds, but equally, regions with strong fields and no folds, illustrating that such structures need not be volume filling. Moreover, the ‘spontaneous stochasticity’, that applies to highly turbulent flows (Eyink 2011), suggests that the dynamics of small-scale dynamos could be quite different in turbulent compared to laminar high- Pr_M systems. Furthermore, in galaxy clusters the viscosity may be set by plasma effects (Schekochihin et al. 2005a). It could also be highly anisotropic owing to the presence of magnetic fields (Parrish et al. 2012). In addition, heat condition is also very anisotropic, giving rise to magnetothermal and heat flux-driven buoyancy instabilities (Parrish and Stone 2005; Parrish and Quataert 2008). Further work on these aspects is desirable, using both semi-analytical ideas and high resolution simulations.

2.2 Low magnetic Prandtl number

In many astrophysical settings, like solar, stellar, or accretion disk plasmas, the magnetic Prandtl number is rather low ($\sim 10^{-4}$ or less). This becomes numerically hard to handle, especially if the magnetic Reynolds number should still be large enough to support dynamo action. In Figure 4 we compare non-helical and helical runs with

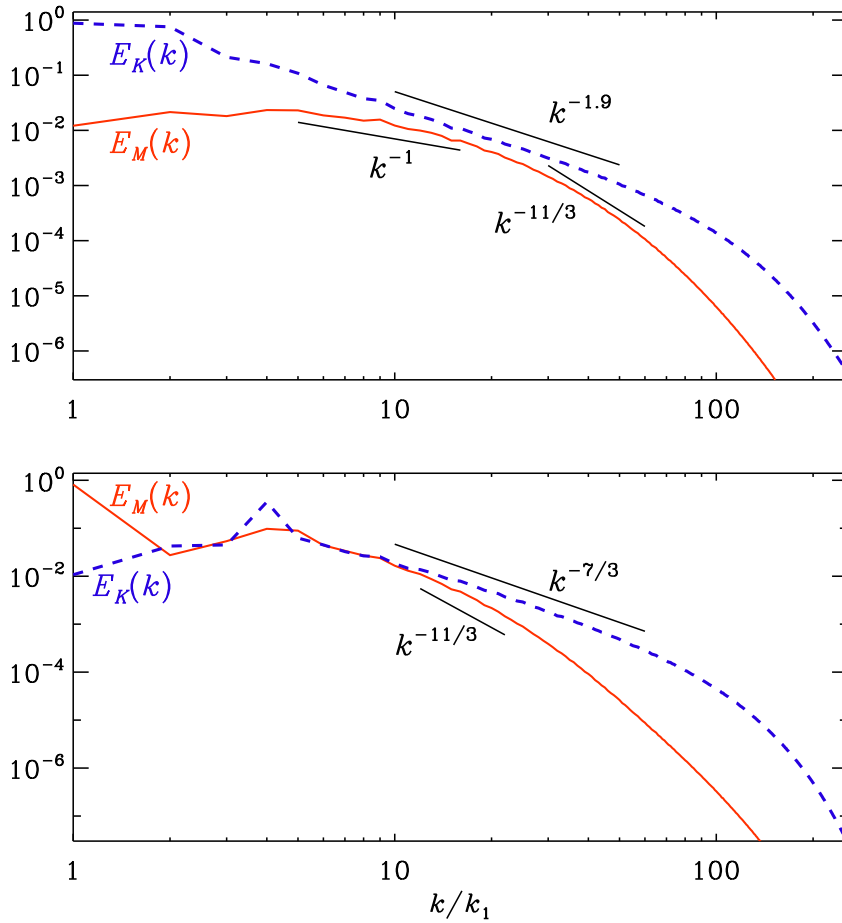


Fig. 4 Kinetic and magnetic energy spectra for non-helical (top) and helical (bottom) turbulence at low magnetic Prandtl numbers of $\text{Pr}_M = 0.02$ and 0.01 , respectively. Here, $\text{Re}_M = 230$ with $\text{Re} = 11,500$ in the non-helical case, adapted from Brandenburg (2011a), and $\text{Re}_M = 23$ with $\text{Re} = 2300$ in the helical case adapted from Brandenburg (2009). In both cases the resolution is 512^3 mesh points.

magnetic Prandtl numbers of 0.02 and 0.01 , respectively. In the former case the magnetic Reynolds number Re_M is 230 , which is weakly supercritical; the critical value of Re_M for small values of Pr_M is $R_{m,\text{crit}} \approx 150$ (Brandenburg 2011a), compared with $R_{m,\text{crit}} \approx 35$ for $\text{Pr}_M = 1$ (Haugen et al. 2004). These values agree with those of earlier work (Schekochihin et al. 2005b, 2007; Iskakov et al. 2007). So, for $\text{Re}_M = 230$ and $\text{Pr}_M = 0.02$, we have $\text{Re} = \text{Re}_M/\text{Pr}_M = 11,500$. Normally, this would require a numerical resolution of about $10,000^3$ meshpoints, but it turns out that at low values of Pr_M , most of the energy is dissipated resistively, leaving thus very little kinetic energy to be cascaded, terminating therefore the kinetic energy cascade earlier than at $\text{Pr}_M = 1$.

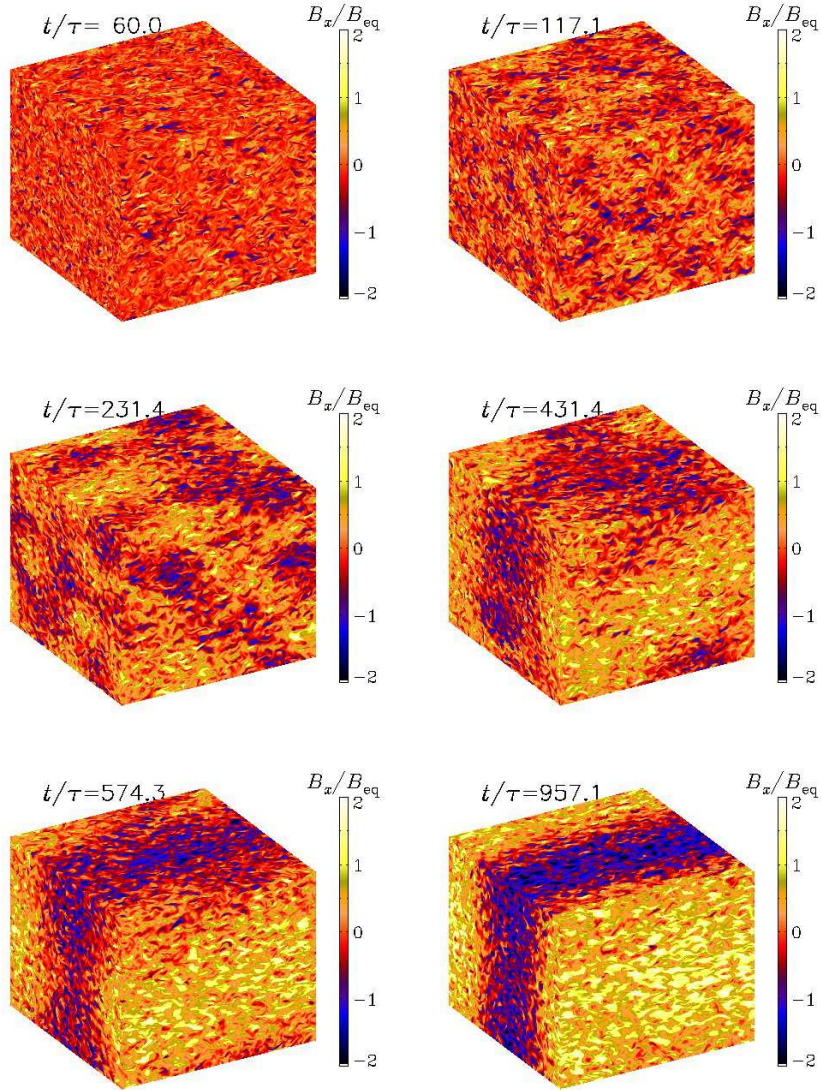


Fig. 5 Visualizations of B_x/B_{eq} on the periphery of the domain at six times during the late saturation stage of the dynamo when a large-scale field is gradually building up. The small-scale field has reached its final value after $t/\tau \approx 100$ turnover times. Here, $B_{\text{eq}} = \sqrt{\mu_0 \rho_0} u_{\text{rms}}$ is the equipartition field strength where kinetic and magnetic energy densities are comparable, and ρ_0 is the mean density. Note that the maximum field strength is about twice B_{eq} .

At intermediate length scales, kinetic and magnetic energy spectra are close to each other. The magnetic energy spectrum no longer exceeds the kinetic energy spectrum, as was found for $\text{Pr}_M = 1$; see Figure 1. Again, this might be a consequence of still insufficiently large Reynolds numbers and limited resolution. In fact, it is plausible

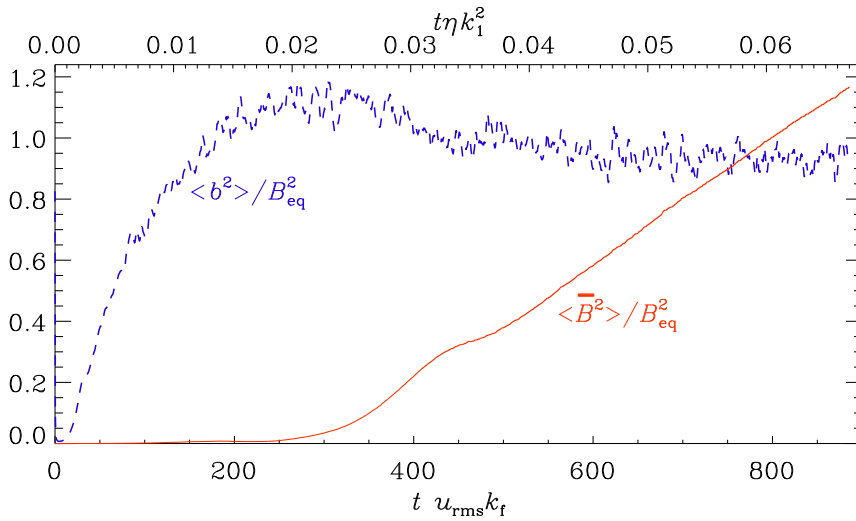


Fig. 6 Saturation of the small-scale magnetic energy density and continued increase of the large-scale magnetic energy density. Here, $k_f/k_1 = 15$.

that, in the limit of large fluid and magnetic Reynolds numbers, kinetic and magnetic energy spectra coincide, even if Pr_M is small. And only at much smaller scales, the magnetic energy spectrum turns into a dissipative subrange, and goes below the kinetic energy spectrum, due to stronger Ohmic dissipation. The slopes of the $k^{-11/3}$ spectrum of Golitsyn (1960) and Moffatt (1961) and the scale-invariant k^{-1} spectrum (Ruzmaikin and Shukurov 1982; Kleeorin and Rogachevskii 1994; Kleeorin et al. 1996) are shown for comparison. However, the kinetic energy spectrum tends to be steeper than $k^{-5/3}$ and is closer to $k^{-1.9}$ and $k^{-7/3}$ in the non-helical and helical cases.

2.3 Inverse transfer and α effect

The dynamics of a large-scale dynamo is most dramatic when the scale separation ratio is large, i.e., $k_f/k_1 \gg 1$. In Figure 1 it was only 4, but now we consider a case where $k_f/k_1 = 15$. In Figure 5 we show visualizations of one component of the field for different times. Evidently, a large-scale field develops that varies in the y direction. This particular large-scale field is best described by xz averages. In Figure 6 we show the evolution of the mean energy density of this large-scale magnetic field, $\langle \overline{B^2} \rangle$, and compare it with that of the small-scale field, $\langle b^2 \rangle = \langle B^2 \rangle - \langle \overline{B^2} \rangle$. Note that the small-scale field reaches its final saturation value during the time span considered, while the large-scale field has not yet saturated and is expected to do so on the diffusive time scale of the box such that $t\eta k_1^2 = O(1)$. It is also interesting to note that the large-scale field starts becoming noticeable only when $t\eta k_1^2 \sim 0.02$, or when $(t/t_d) \sim 4.5$, where $t_d = (\eta k_f^2)^{-1}$ is the resistive timescale at the forcing scale. In other words one needs several resistive (diffusive) times at the forcing scale, before the large-scale field can grow. We will interpret this result below in terms of the resistive dissipation of small-scale magnetic helicity which alleviates α quenching.

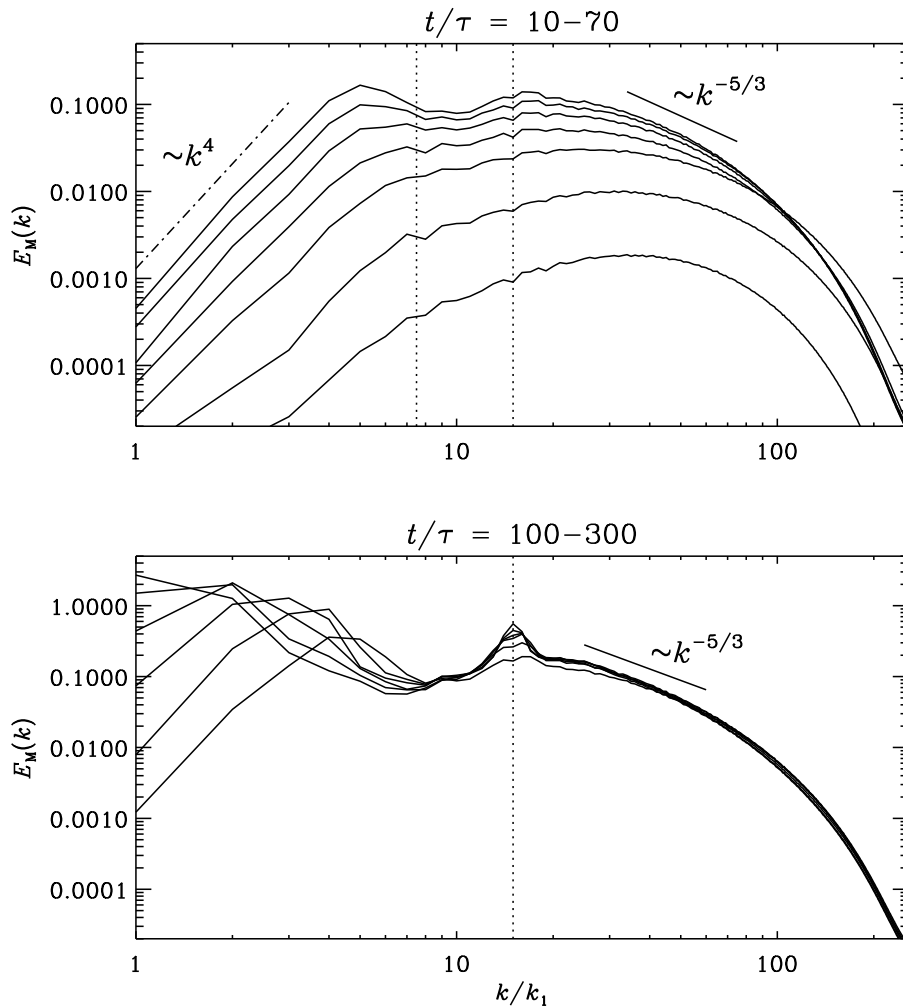


Fig. 7 Magnetic energy spectra $E_M(k)$, at earlier (top) and later (bottom) times. The scale separation ratio is $k_f/k_1 = 15$. The range of time t is given in units of the turnover time, $\tau = 1/u_{\text{rms}}k_f$. At small wavenumbers, the $E_M(k)$ spectrum is proportional to k^4 , while to the right of $k_f/k_1 = 15$ there is a short range with a $k^{-5/3}$ spectrum.

The evolution of the magnetic energy spectrum for this case is shown in Figure 7, where we see several stages during the early phase of the dynamo, and in a separate panel the later saturation behavior. Clearly, a large-scale field is already present for $t/\tau > 100$, but the field is then still fairly isotropic and therefore not very pronounced in visualizations shown in Figure 5. Spectra of magnetic energy and rescaled magnetic helicity are shown in Figure 8 for the saturated state. Here, magnetic helicity spectra $H_M(k)$ are normalized such that $\int H_M dk = \langle \mathbf{A} \cdot \mathbf{B} \rangle$, where $\mathbf{B} = \nabla \times \mathbf{A}$ is the magnetic field expressed in terms of its vector potential. Note that at early times, the magnetic field shows the Kazantsev $k^{3/2}$ slope ($t/\tau = 10$) in the range $7 \leq k/k_1 \leq 25$. However,

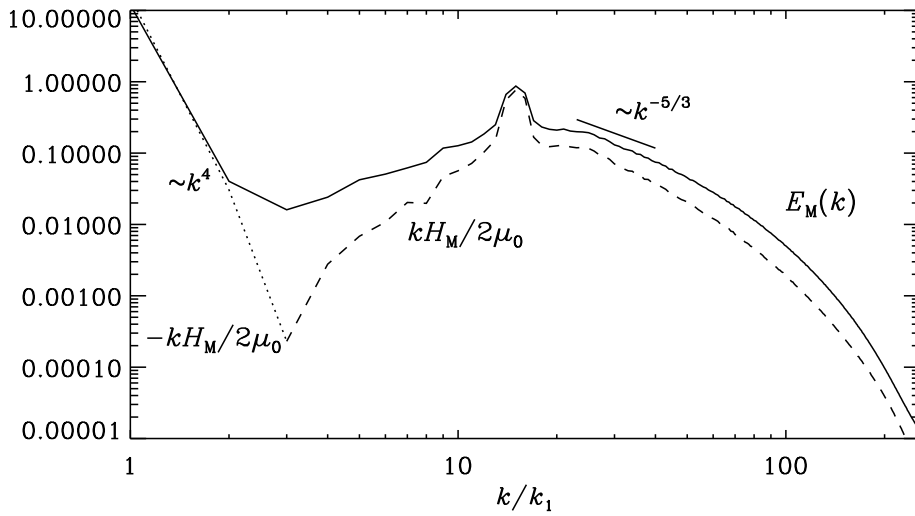


Fig. 8 Spectra of magnetic energy, $E_M(k)$, and rescaled magnetic helicity, $\pm kH_M(k)/2\mu_0$.

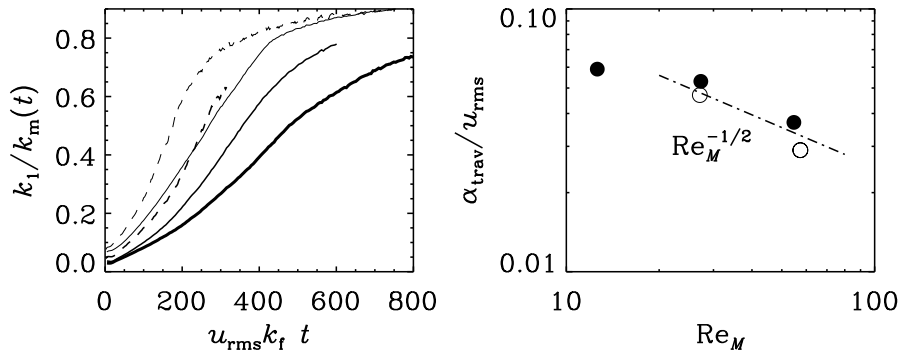


Fig. 9 Left panel: time dependence of the peak wavenumber for scale separation ratios of 15 (dashed) and 30 (solid lines) at Re_M of 12, 27, and around 57 (increasing line thickness). Right panel: Re_M dependence of the cascade speed for scale separation ratios of 15 (open symbols) and 30 filled symbols. The straight lines give the $Re_M^{-1/2}$ (dotted) and Re_M^{-1} (dashed) dependences. Adapted from Brandenburg (2011b).

already at times $t/\tau = 20$ and 30 one sees a small hump at $k_f/2$, which is significant in view of an interpretation of these results in terms of a so-called α^2 dynamo, which will be discussed in Section 2.4.

The temporal increase of the typical scale of the large-scale field can be determined by monitoring the quantity

$$\ell_m(t) \equiv k_m^{-1}(t) = \int k^{-1} E_M(k) dk \Big/ \int E_M(k) dk. \quad (3)$$

In Figure 9 we plot $k_m^{-1}(t)$ for different values Re_M . Here, we normalize with respect to the minimal wavenumber $k_1 = 2\pi/L$ in the domain of size L , so we plot k_1/k_m .

There is a limited scaling range that allows us to determine the increase of $\ell_m(t)$ for different values of Re_M . We measure the speed at which the bump travels toward larger scales by the quantity $\alpha_{\text{trav}} = d\ell_m/dt$. In the right-hand panel of Figure 9 we plot the resulting values of α_{trav} as a function of Re_M . The results are compatible with a resistively limited increase whose speed diminishes like $\text{Re}_M^{-1/2}$. This behavior was first seen in simulations of Brandenburg et al. (2002) and then more convincingly at larger resolution in simulations of Brandenburg (2011b). Such a behavior further reinforces our earlier remark that the large-scale field can only grow on the slow resistive timescale in periodic boxes.

2.4 Connection with mean-field theory

There exists a close analogy between the inverse transfer described above and mean-field dynamo theory in that both are able to predict the occurrence of large-scale fields with similar properties and excitation conditions. In mean-field theory one splits the velocity field \mathbf{U} and magnetic field \mathbf{B} into the sum of a mean, large-scale components ($\overline{\mathbf{U}}$ and $\overline{\mathbf{B}}$) and a turbulent, stochastic components (\mathbf{u} and \mathbf{b}); that is $\mathbf{U} = \overline{\mathbf{U}} + \mathbf{u}$ and $\mathbf{B} = \overline{\mathbf{B}} + \mathbf{b}$. One then solves the averaged induction equation,

$$\frac{\partial \overline{\mathbf{B}}}{\partial t} = \nabla \times (\overline{\mathbf{U}} \times \overline{\mathbf{B}} + \overline{\mathcal{E}} - \eta \mu_0 \overline{\mathbf{J}}), \quad (4)$$

where $\overline{\mathcal{E}} = \overline{\mathbf{u} \times \mathbf{b}}$ is the mean electromotive force that we discussed already in connection with Equation (1). Under the assumption of isotropy and sufficient scale separation in space and time, we have just $\overline{\mathcal{E}} = \alpha \overline{\mathbf{B}} - \eta_t \mu_0 \overline{\mathbf{J}}$, where α and η_t are a pseudo-scalar and a scalar respectively. For the case when there is no mean flow, a stability analysis gives the dispersion relation for the growth rate λ as

$$\lambda = \alpha k - (\eta_t + \eta) k^2, \quad (5)$$

and the eigenfunctions are force-free solutions with $\eta_t \mu_0 \overline{\mathbf{J}} = \alpha \overline{\mathbf{B}}$, which are plane polarized waves, just like in Figure 5, where the large-scale field can be approximated by $\overline{\mathbf{B}} \propto (\sin ky, 0, \cos ky)$, ignoring here an arbitrary phase shift in the y direction. The dynamo is excited when $C_\alpha \equiv \alpha/(\eta_t + \eta)k > 1$, where C_α is the relevant dynamo number in this context. The fastest growing mode occurs at wavenumber $k = k_{\text{max}} = \alpha/[2(\eta_t + \eta)]$. Furthermore, using estimates for the high-conductivity limit,

$$\alpha = \alpha_K = -\frac{1}{3}\tau \langle \boldsymbol{\omega} \cdot \mathbf{u} \rangle \quad \text{and} \quad \eta_t = \frac{1}{3}\tau \langle \mathbf{u}^2 \rangle, \quad (6)$$

we find that $C_\alpha = \epsilon_f k_f / k_1$ (Brandenburg et al. 2002), where $\epsilon_f \leq 1$ is the fractional helicity, and $\eta \ll \eta_t$ has been assumed. We can now return to our discussion in connection with Figure 7, where we notice that at early times the field growth occurs at wavenumber $k_f/2$. This is indeed the value expected from our simple estimate, since for fully helical turbulence, we expect $\langle \boldsymbol{\omega} \cdot \mathbf{u} \rangle = k_f \langle \mathbf{u}^2 \rangle$, and thus $k_{\text{max}} = \alpha/2\eta_t = k_f/2$.

It is of interest at this point to comment on the validity of mean-field dynamo concepts. In condensed matter physics for example mean-field theory is generally valid when applied to systems where fluctuations are assumed small. In high Re_M turbulent systems on the other hand, the fluctuations grow more rapidly than the mean-field, due to small scale dynamo action. Thus, even in the kinematic stage when Lorentz forces

are small, one needs a closure theory to calculate the mean-field turbulent coefficients like α and η_t . Traditionally these coefficients have been derived by still making a quasi-linear approximation (strictly valid for small fluctuating fields), which is also known as the first order smoothing approximation (FOSA) (Moffatt 1978; Krause and Rädler 1980; Brandenburg and Subramanian 2005a). This is sometimes also referred to as the second order correlation approximation. Some improvements to this can be made by adopting closure approximations like the minimal tau approximation whereby triple correlations involving fluctuating fields are taken to provide a damping term proportional to the quadratic correlations (Blackman and Field 2002; Rädler et al. 2003; Brandenburg and Subramanian 2005a). There are also a few cases, like δ correlated flows (Kazantsev 1967; Zeldovich et al. 1983) or renovating flows (Dittrich et al. 1984; Gilbert and Bayly 1992) which provide analytically solvable models, where the form of α and η_t given by Equation (6) is recovered.

In this context, direct simulations as discussed above, which can be interpreted in terms of mean-field concepts, lend some validity to the theory. This applies also to the interpretation of results in the nonlinear regime to be discussed below. Moreover, when the α and η_t have been measured directly in simulations of isotropic turbulence, one gets results remarkably close to the estimates of FOSA given in Equation (6) (Sur et al. 2008). This suggests that the strong magnetic field fluctuations produced by small-scale dynamo action do not contribute a systematic large-scale component to the mean emf $\overline{\mathcal{E}} = \overline{\mathbf{u} \times \mathbf{b}}$, correlated with the mean field. They do make the mean-field coefficients noisy. However, the fact that we can still use the mean-field concept in understanding the results of direct simulations implies that this noise does not have a crucial effect, perhaps after the small-scale dynamo has nearly saturated. The saturation of the dynamo will be discussed further in Section 2.6.

2.5 Shear dynamos

Remarkably, not all large-scale dynamos require an α effect. In fact, large-scale dynamo action has been seen in simulations with just shear and no helicity; see Brandenburg (2005a) for simulations using a shear profile motivated by that of the Sun. An obvious candidate at the time was the so-called shear-current effect (Rogachevskii and Kleeorin 2003, 2004), which requires $\eta_{ij}\overline{U}_{i,j} > 0$, where η_{ij} is the part of the magnetic diffusivity tensor that multiplies $\overline{\mathbf{J}}$ such that $\overline{\mathcal{E}}_i = \dots - \eta_{ij}\overline{J}_j$, and $\overline{U}_{i,j}$ is the velocity shear. Already early calculations using the test-field method showed that the relevant component of η_{ij} has the wrong sign (Brandenburg 2005b). This confirmed the results of quasilinear calculations (Rädler and Stepanov 2006; Rüdiger and Kitchatinov 2006; Sridhar and Singh 2010; Singh and Sridhar 2011). Moreover in the large Re_M limit using FOSA, but for arbitrarily strong shear, the corresponding cross coupling implied by the shear current effect was shown to be absent (Sridhar and Subramanian 2009a, 2009b). The issue of how the mean-field grows in nonhelical turbulence in the presence of shear remained open in view of other possible contenders.

One possibility is the incoherent α -shear dynamo that lives from the combination of shear and fluctuations of the α effect and was originally invoked by Vishniac and Brandenburg (1997) to explain the magnetic field of unstratified shearing box simulations of accretion disc turbulence (Hawley et al. 1995). This mechanism has received considerable attention in the following years (Sokolov 1997; Silant'ev 2000; Fedotov et al. 2006; Proctor 2007; Kleeorin and Rogachevskii 2008; Sur and Subramanian 2009). Meanwhile, ev-

idence for the existence of shear dynamos in simple shearing box simulations was mounting (Yousef et al. 2008a,2008b; Brandenburg et al. 2008; Herault et al. 2011). Although the underlying mechanism may have appeared to be a new one, there is now quantitative evidence that this can be explained by an incoherent α -shear dynamo (Brandenburg et al. 2008; Heinemann et al. 2011; Mitra and Brandenburg 2012). This is remarkable given the unconventional nature of the approach whereby one uses mean-field theory over two spatial directions and considers the fluctuations that remain in time and the third coordinate direction as physically meaningful.

2.6 α -quenching

A fully satisfactory theory for the magnetic feedback on the α effect does not exist. What we do know is that for strong mean fields $\overline{\mathbf{B}}$, this α becomes a tensor of the form $\alpha_{ij} = \alpha_1(\overline{B})\delta_{ij} - \alpha_2(\overline{B})\hat{B}_i\hat{B}_j$, where $\hat{\mathbf{B}} = \overline{\mathbf{B}}/\overline{B}$ are unit vectors, and $\overline{B} = |\overline{\mathbf{B}}|$ is the modulus. However, if this tensor is applied to the $\overline{\mathbf{B}}$ field, we have $\alpha_{ij}\overline{B}_j = (\alpha_1 - \alpha_2)\overline{B}_i$, which suggests that α is just like a scalar. We also know that at least part of the quenching acts in such a way that the total field (small-scale and large-scale) obeys the magnetic helicity evolution equation. This was derived some time ago in a certain approximation by Pouquet et al. (1976) and was then applied to derive an equation for the quenching of α (Kleeorin and Ruzmaikin 1982; Gruzinov and Diamond 1994; Kleeorin et al. 2000; Field and Blackman 2002; Blackman and Brandenburg 2002; Subramanian 2002; Brandenburg and Subramanian 2005a).

The crucial starting point is the realization of Pouquet et al. (1976) that under the influence of Lorentz forces, the α effect has an additional component, $\alpha_M = \frac{1}{3}\tau\overline{\mathbf{j}} \cdot \overline{\mathbf{b}}/\rho_0$, where $\overline{\mathbf{j}} \cdot \overline{\mathbf{b}}$ is the current helicity associated with the small-scale field and $\alpha = \alpha_K + \alpha_M$ is the sum of kinetic and magnetic α effects. Interestingly, Pouquet et al. (1976) also showed that η_t does not get renormalized under the same approximation. Under locally isotropic conditions, in the Coulomb gauge, $\overline{\mathbf{j}} \cdot \overline{\mathbf{b}}$ can be approximated by $k_f^2\overline{\mathbf{a}} \cdot \overline{\mathbf{b}}/\mu_0$, where $\overline{\mathbf{a}} \cdot \overline{\mathbf{b}} \equiv \overline{h}_f$ is the magnetic helicity of the small-scale fields. In order to write an evolution equation for the magnetic helicity density one can fix a gauge for the vector potential. One could also work in terms of the evolution equation for the current helicity (Subramanian and Brandenburg 2004). Perhaps more elegant is to write this evolution in terms of a gauge invariant magnetic helicity density, defined as the density of correlated links of \mathbf{b} , and which is most closely related to the \overline{h}_f in the Coulomb gauge (Subramanian and Brandenburg 2006). The evolution equation for \overline{h}_f is

$$\frac{\partial \overline{h}_f}{\partial t} = -2\overline{\mathcal{E}} \cdot \overline{\mathbf{B}} - 2\eta k_f^2 \overline{h}_f - \nabla \cdot \overline{\mathbf{F}}_f, \quad (7)$$

where $\overline{\mathbf{F}}_f$ is the magnetic helicity flux of the small-scale field. This equation shows that the α effect produces magnetic helicity at a rate $-2\overline{\mathcal{E}} \cdot \overline{\mathbf{B}} = -2\alpha_{\text{red}}\overline{\mathbf{B}}^2$, where $\alpha_{\text{red}} = \alpha - \eta_t k_m$ is the reduced α effect and $k_m = \mu_0\overline{\mathbf{J}} \cdot \overline{\mathbf{B}}/\overline{\mathbf{B}}^2$ is the effective wavenumber of the mean field. In a supercritical dynamo, the sign of α_{red} agrees with that of α (the η_t term is subdominant). Then starting with a specific sign for the kinetic α_K and zero magnetic α_M , this produces α_M of opposite sign, which quenches the total α and the dynamo progressively with increasing field strength. In the absence of a magnetic helicity flux, this process happens on a resistive time scale, which is what is seen in Figure 6, where final saturation is not even remotely in sight. We recall that a rapid

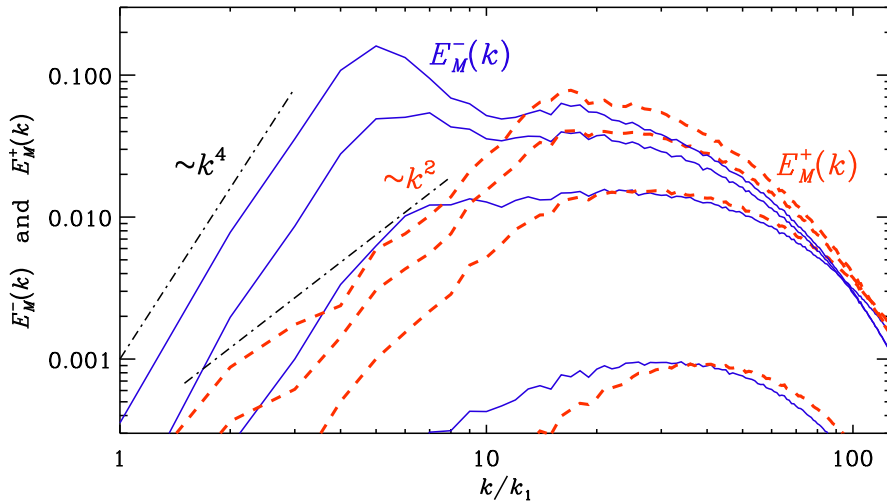


Fig. 10 Magnetic energy spectra $E_M^\pm(k)$ of positively (red) and negatively (blue) polarized parts at earlier times. Note the preferred build-up of the large-scale field at $E_M^-(k_f/2)$, relative to the slower growth of $E_M^+(k_f)$. Slopes proportional to k^2 for E_M^+ and k^4 for E_M^- are shown.

evolution of the energy of the mean field up to k_1/k_f times the equipartition value is expected on theoretical grounds (Blackman and Brandenburg 2002). In practice, this is hard to verify because at early times the mean field has not yet reached the scale of the system and modes of different orientation are still competing. Nevertheless, by splitting the magnetic field into its positively and negatively polarized contributions, $E_M^\pm(k) = \frac{1}{2}[E_M(k) \pm kH_M(k)]$, it is possible to separate large-scale and small-scale fields (Brandenburg et al. 2002; Brandenburg and Subramanian 2005a; Brandenburg 2011b). In Figure 10 we clearly see a faster build-up of the large-scale field through $E_M^-(k)$ compared with the small-scale field through $E_M^+(k)$. As we have argued before, this build-up of large-scale fields is still resistively slow, but it is important to realize that the demonstrated existence of large-scale fields in the kinematic stage provides support for the usefulness of the mean-field approach.

The final saturation value, in periodic box simulations, can be estimated simply by noting that in the absence of magnetic helicity fluxes, the total current helicity must vanish in the steady saturated case, i.e., $\overline{\mathbf{J} \cdot \mathbf{B}} + \overline{\mathbf{j} \cdot \mathbf{b}} = 0$. This is because the total current helicity drives the change of magnetic helicity, which in steady state must be zero. Such a state can be obtained in a nontrivial manner with helical forcing when current helicity has opposite signs at large and small length scales. For example, if the kinetic helicity at small scales is positive (that is α_K is negative), then the generated α_M is positive. In that case the current helicity of small-scale fields is also positive with $\mu_0 \overline{\mathbf{j} \cdot \mathbf{b}} = k_f \overline{\mathbf{b}^2}$ and hence $\mu_0 \overline{\mathbf{J} \cdot \mathbf{B}} = -k_1 \overline{\mathbf{B}^2}$ is negative. (This implies that $k_m = -k_1$.) Assuming furthermore equipartition between kinetic and magnetic energies at small scales, i.e., $\overline{\mathbf{b}^2} \approx \mu_0 \overline{\rho \mathbf{u}^2} \equiv B_{\text{eq}}^2$, we obtain (Brandenburg 2001)

$$\overline{\mathbf{B}^2}/B_{\text{eq}}^2 \approx k_f/k_1 \quad (8)$$

in the final state. We recall that in the run shown in Figure 6, the scale separation ratio is $k_f/k_1 = 15$, so it is understandable that there is not yet any sign of saturation of the large-scale field; see Brandenburg (2001) for early results on the resistively slow saturation.

We do not expect resistively slow saturation behavior to occur in stars or galaxies, because the $\nabla \cdot \overline{\mathbf{F}}_f$ term can usually not be neglected (Blackman and Field 2000a, 2000b; Kleorin et al. 2000; Brandenburg and Subramanian 2005b; Shukurov et al. 2006). These results were obtained by solving the mean-field equations. Subsequent simulations have shown that turbulent diffusive fluxes exist that would constitute a sufficient contribution to $\nabla \cdot \overline{\mathbf{F}}_f$ (Mitra et al. 2010; Hubbard and Brandenburg 2010), especially when Re_M is larger than a critical value around 10^4 . This flux term can then dominate over the $2\eta\overline{\mathbf{j}} \cdot \overline{\mathbf{b}}$ term (Candelaresi et al. 2011). Under certain considerations it is possible that a flux of the form $\overline{\mathcal{E}} \times \overline{\mathbf{A}}$ from the mean electromotive force contributes to the flux term, but by solving an evolution equation for the magnetic helicity density of the total (small- and large-scale) field, consideration of this term can be avoided. This approach is also suited to deal with fluxes associated with gauges that can introduce artificial fluxes in shearing environments; see Hubbard and Brandenburg (2011). They find no evidence for a flux resulting from shear that were previously argued to be important (Vishniac and Cho 2001). Using simulations with anisotropic non-helical forcing in the presence of shear, Shapovalov and Vishniac (2011) argue that large-scale dynamos might even live entirely due to helicity fluxes, although the exact origin of this flux remains to be clarified. Another natural contribution to the flux term is just advection of both small-scale and large-scale fields, along with the associated magnetic helicity (Shukurov et al. 2006; Subramanian and Brandenburg 2006). This will naturally arise from coronal mass ejections in the solar context, or supernovae driven outflows in galaxies (Blackman and Brandenburg 2003; Shukurov et al. 2006; Sur et al. 2007; Warnecke et al. 2011).

Large-scale dynamos therefore seem to need helicity fluxes to work efficiently. This conclusion can be understood more physically as follows. As the large-scale mean field grows, the turbulent emf $\overline{\mathcal{E}}$ is transferring helicity between the small- and large-scale fields. The large-scale helicity is in the links of the mean poloidal and toroidal fields of the astrophysical system like the Sun or the Galaxy, while the small-scale helicity is in what can be described as ‘twist helicity’ (or simply twist) of the small-scale field, produced by helical motions. Lorentz forces associated with the ‘twisted’ small-scale field would like to untwist the field. This would lead to an effective magnetic α_M effect which opposes the kinetic α_K produced by the helical turbulence. The cancellation of the total α effect can lead to catastrophic quenching of the dynamo. This quenching can be avoided if there is some way of dissipating the twist (which is slow in high- Re_M system) or transferring the twists in the small-scale field out of the region of dynamo action, or cancelling it between two hemispheres. That is, if there are helicity fluxes out of the system or between different parts of the system, the large-scale field can grow to observable strengths.

2.7 Application of mean-field theory to galaxies

The mean-field theory described above has been applied extensively to understand magnetic fields of disk galaxies. The mean-field dynamo equations allow substantial simplification provided a suitable parameterization of turbulent transport coefficients

is chosen. Of course, this parameterization presumes a suitable closure for nonlinear effects to arrive at a closed set of nonlinear mean-field dynamo equations. Such an approach does not necessarily imply a deep understanding of the physical processes involved in the magnetic field evolution. However, it appears to be sufficient for pragmatic modeling of magnetic field configurations in particular galaxies to be compared with the observational data of polarized radio emission.

A first example of such parameterization and further drastic simplification of mean-field dynamo equations was presented by Parker (1955). Early simplified models for the galactic dynamo, which allow analytic or quasi-analytic investigations, can be found in Ruzmaikin et al. (1988), and more recent reviews by Beck et al. (1996), Shukurov (2004), and Kulsrud and Zweibel (2008). Next, one can suggest, as the most pragmatic contender, simple mean-field model for galactic dynamo the so-called no- z model (Subramanian and Mestel 1993; Moss 1995). The idea of this model is to present azimuthal and radial components of the mean galactic magnetic field by their quantities at the galactic equator and average the mean-field equations with respect to the coordinate z perpendicular to the galactic plane. The third component of the magnetic field can be reconstructed from the condition $\text{div} \overline{\mathbf{B}} = 0$. This approach is an obvious oversimplification, but it appears still adequate for modeling magnetic field evolution including the helicity fluxes discussed above (Sur et al. 2007; Chamandy et al. 2012). It also allows one to model magnetic configurations for design studies of new generations of radio telescopes such as the Square Kilometer Array; cf. Moss et al. (2012).

2.8 Application to mean-field dynamos of stars and the Sun

In comparison with galactic dynamos, the status of the theory of solar and stellar dynamos is less satisfactory. Early models by Steenbeck and Krause (1969) provided numerical solutions to the full two-dimensional axisymmetric mean-field equations under the assumption of an assumed profile of the internal angular velocity $\Omega(r, \theta)$, whose radial gradient, $\partial\Omega/\partial r$, was negative, and variations in colatitude θ were ignored in most of their models. This yielded cyclic magnetic fields with equatorward migration under the assumption that the α effect is predominantly positive in the northern hemisphere. Subsequently, helioseismology delivered detailed contours of $\Omega(r, \theta)$, which excluded the previously assumed Ω profiles and suggested that $\partial\Omega/\partial r > 0$ at low latitudes where strong magnetic flux belts are observed to propagate equatorward during the course of the 11 year sunspot cycle.

Various solutions have been offered to this dilemma (Parker 1987). The most prominent one is the flux transport dynamo (Choudhuri et al. 1995; Dikpati and Charbonneau 1999), whereby meridional circulation causes the dynamo wave to turn around in the opposite direction. This model operates under the assumption that the turbulent magnetic diffusivity operating on the toroidal field is much lower than the value suggested by mixing length theory, and the α effect is assumed to work only at the surface. The other proposal is that the dynamo wave obeys equatorward migration owing to a narrow near-surface shear layer (Brandenburg 2005a), where $\partial\Omega/\partial r$ is indeed strongly negative; see Fig. 4 of Benevolenskaya et al. (1999). This proposal still lacks detailed modeling. In view of the shortcomings in the treatment of mean-field dynamo theory (e.g., our ignorance concerning nonlinearity discussed in Section 2.6 or the neglect of finite scale separation discussed below in Section 2.10), the ground for speculation remains fertile. Magnetic helicity fluxes in interface and flux transport dynamos have

already been looked at (Chatterjee et al. 2010), but finite scale separation effects are neglected. Indeed, the Sun is strongly stratified with its scale height changing rapidly with depth, making it hard to imagine that simple-minded approaches that ignore this can be meaningful at all. A cornerstone for the proposal that solar activity is a shallow phenomenon may lie in the success of explaining the formation of active regions and perhaps even sunspots as a result of spontaneous formation of flux concentrations by convective flux collapse (Kitchatinov and Mazur 2000) or the negative effective magnetic pressure instability; see Section 2.11 below.

2.9 Magnetic helicity in the solar dynamo exterior

There is now explicit evidence for the presence of magnetic helicity in the exterior of dynamos. In particular, it has been possible to detect magnetic helicity of opposite signs at small and large length scales. This has been possible through measurements of magnetic helicity spectra in the solar wind away from the equatorial plane (Brandenburg et al. 2011). This data pointed for the first time to a *reversal* of magnetic helicity density between interior and exterior of the dynamo. Such reversals have now been confirmed in numerical simulations of dynamos coupled to an exterior. There are first of all the simulations of Warnecke et al. (2011) showing coronal mass ejections from a turbulent dynamo in a wedge of a spherical shell, where the reversal occurred some distance away from the dynamo. Next, there are related simulations in Cartesian geometry where a reversal can be found immediately above the surface; see figure 12 of Warnecke and Brandenburg (2010). Finally, there are earlier mean-field simulations showing such a reversal as well; see the lower panel of figure 7 of Brandenburg et al. (2009).

The occurrence of such a reversal is now well understood in terms of the magnetic helicity equation for the small-scale field shown in Equation (7). In the dynamo interior, the α effect dominates over turbulent magnetic diffusion and produces magnetic helicity of a sign opposite to that of α . In the northern hemisphere, α is positive, so this produces negative \overline{h}_f . Turbulent magnetic diffusivity opposes this effect, but it is still subdominant and can therefore not change the sign of \overline{h}_f . This is different in the solar wind where the α becomes subdominant compared with turbulent diffusion, which is the reason the sign of \overline{h}_f is now different (Brandenburg et al. 2011).

2.10 Scale separation in space and time

In connection with Equation (1) we noted that the relation between $\overline{\mathcal{E}}$ and $\overline{\mathcal{B}}$ does, in general, involve a convolution in space and time. This becomes important when the variations of $\overline{\mathcal{B}}$ occur on time and length scales comparable with those of the turbulence, whose turnover time is ℓ/u_{rms} and its typical scale is $\ell = k_f^{-1}$. The properties of the integral kernel are often determined in Fourier space, in which case a useful approximation of it is $\hat{\alpha}_{ij}(k, \omega) = \alpha_{ij}^{(0)} \hat{K}(k, \omega)$ and $\hat{\eta}_{ijk}(k, \omega) = \eta_{ijk}^{(0)} \hat{K}(k, \omega)$, where

$$\hat{K}(k, \omega) = \frac{1}{1 - i\omega\tau + k^2\ell^2}. \quad (9)$$

Such an integral kernel has recently been obtained with the test-field method applied to passive scalar diffusion (Rheinhardt and Brandenburg 2012), and in limiting cases (either with $\omega = 0$ or with $k = 0$) for α and η_t ; see Brandenburg et al.

(2008) and Hubbard and Brandenburg (2009) for details and applications to spatial and temporal nonlocalities, respectively. The test-field method allows one to determine the turbulent transport coefficients by solving an extra set of equations that describe the evolution of the fluctuating magnetic field for each test field, which is a predetermined mean field. Under some conditions it is also necessary to solve corresponding evolution equations for velocity perturbations (Rheinhardt and Brandenburg 2010). The combined presence of spatio-temporal nonlocality was first considered by (Rheinhardt and Brandenburg 2012), who proposed Equation (9) and used it to reformulate Equation (1) as a simple differential equation of the form

$$\left(1 + \tau \frac{\partial}{\partial t} - \ell^2 \frac{\partial^2}{\partial z^2}\right) \bar{\mathcal{E}}_i = \alpha_{ij}^{(0)} \bar{B}_j + \eta_{ijk}^{(0)} \bar{B}_{j,k}. \quad (10)$$

Such an equation is quite easy to implement and represents an improvement in terms of physical realism. This representation avoids not only the problem of causality associated with the infinite speed of signal propagation in the absence of the time derivative (Brandenburg et al. 2004), but it also prevents the development of artificially small scales in the mean field.

The application of this new technique is still in its infancy, and it needs to be seen to what extent spatio-temporal nonlocality can substantially alter the nature of the solutions. As an example we note that a finite τ has been found to lower the critical dynamo number for oscillatory solutions by a factor of about 2 (Rheinhardt and Brandenburg 2012). In the context of disk galaxies, such non-locality in time can also lead to phase shifts between the spiral forcing of the dynamo by matter arms, and the resulting magnetic spirals, as seen in the galaxy NGC6946 (Chamandy et al. 2012).

2.11 Magnetic structures resulting from strong density stratification

Finally, let us discuss a mean-field effect that occurs under the condition of strong density stratification. It has been theoretically anticipated long ago (Kleeorin et al. 1993, 1996; Kleeorin and Rogachevskii 1994; Kleeorin et al. 1989, 1990; Rogachevskii and Kleeorin 2007), but only more recently was it also seen in numerical simulations of the mean-field equations (Brandenburg et al. 2010) and then in direct numerical simulations (Brandenburg et al. 2011; Kemel et al. 2012).

The essence of this effect is the suppression of turbulent intensity by a mean magnetic field. This means that the effective pressure caused by $\bar{\mathbf{B}}$ is not just $\bar{\mathbf{B}}^2/2\mu_0$, but there must also be an additional contribution from the suppression of the turbulence, which leads to a negative contribution (Kleeorin et al. 1989, 1990; Kleeorin and Rogachevskii 1994; Kleeorin et al. 1996; Rogachevskii and Kleeorin 2007). This modifies the nature of the magnetic buoyancy instability in such a way that magnetic structures become heavier than their surroundings and sink. This has been demonstrated using both mean-field simulations (Brandenburg et al. 2010) as well as direct numerical simulations (Brandenburg et al. 2011). As an example we show in Figure 11 a snapshot from a direct simulation where a weak ($B_0/B_{\text{eq}0} = 0.01$) magnetic field is imposed in the y direction. The density stratification is isothermal, so the density scale height is constant in the direction of gravity (the negative z direction). The total density contrast from bottom to top is about 540. The instability grows at a rate which scales with $\eta_{t0} k^2$, where $\eta_{t0} = u_{\text{rms}}/3k_f$ is an estimate for the turbulent magnetic diffusivity, which is well reproduced by simulations using the test-field method (Sur et al. 2008).

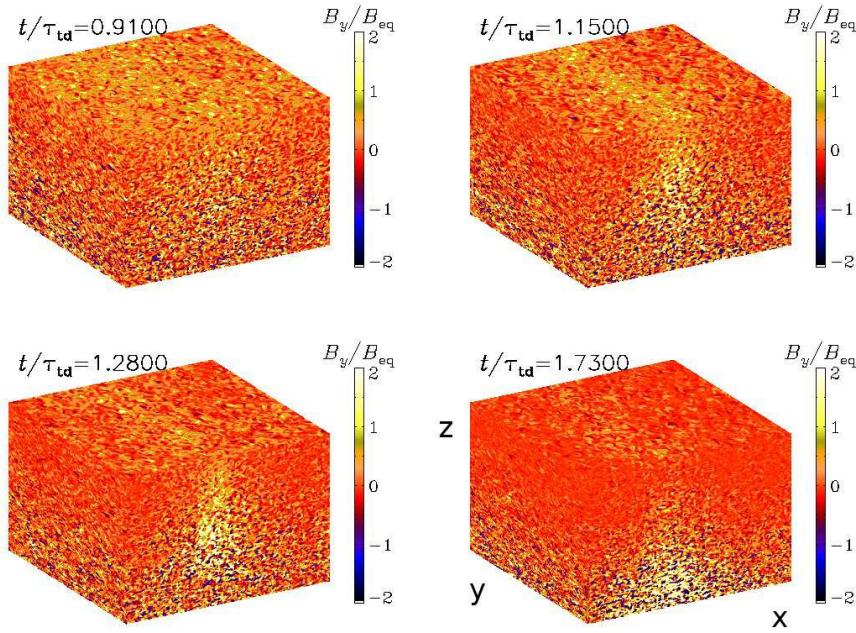


Fig. 11 Visualizations of B_y for a simulation with strong density stratification and a weak imposed magnetic field $(0, B_0, 0)$ with $B_0/B_{eq0} = 0.01$, $Re_M = 18$ and $Pr_M = 0.5$. Time is given in units of turbulent–diffusive times. Note the gradual emergence of a large-scale magnetic flux concentration which then sinks as a result of negative effective magnetic buoyancy. Adapted from Kemel et al. (2012).

The study of this negative effective magnetic pressure is still very much in progress. In particular, it has not yet been studied how this negative effective magnetic pressure instability interacts with the mean-field dynamo. It is envisaged that this instability might produce local magnetic field enhancements in the surface layers that resemble active regions. Such regions are long lived ($\sim 1/2$ year). Traditionally such long timescales have not been associated with the surface layers. However, the time scale of the negative effective magnetic pressure instability is the turbulent–diffusive time, $\tau_{td} = (\eta_{t0} k_1^2)^{-1}$, where $\eta_{t0} = u_{rms}/3k_f$ is the estimated turbulent magnetic diffusivity. This time can be much longer than the local turnover time, $\tau_{to} = (u_{rms} k_f)^{-1}$, which is about (1 day at the bottom of the near-surface shear layer at 40 Mm depth). The ratio of these time scales is $\tau_{td}/\tau_{to} = 3(k_f/k_1)^2$, which can be around 300 for a scale separation ratio of just 10.

In the rest of this paper we focus on small-scale magnetic fields that occur over a range of different astrophysical settings. They are believed to be important in understanding small-scale magnetic fields in the surface layers of the Sun, although that part of the field might also be a consequence of tangling the large-scale magnetic field. Another possible astrophysical application of small-scale dynamos might be the clusters of galaxies, because in the absence of rotation it is difficult to motivate any form of large-scale dynamo action.

3 Analytical approaches to small-scale turbulent dynamos

Direct numerical simulations are now the most straightforward way to understand turbulent dynamos. However, more traditional analytical methods provide a useful support for them. Analytic methods have provided particular insights both into large-scale and small-scale dynamos. We discuss some specific analytic considerations of small-scale dynamos further below.

3.1 Correlation tensor and small-scale dynamo

A natural approach here is to introduce the second-order correlation tensor of the magnetic field $B_i(\mathbf{x}, t)$ as

$$\mathcal{B}_{ij}(\mathbf{x}, \mathbf{y}, t_1, t_2) = \langle B_i(\mathbf{x}, t_1) B_j(\mathbf{y}, t_2) \rangle, \quad (11)$$

taken at two spatial points \mathbf{x} and \mathbf{y} and at two instants t_1 and t_2 . Here $\langle \dots \rangle$ denotes averaging over an ensemble of turbulent velocity field fluctuations which can be described by the velocity field correlation tensor $\mathcal{V}_{ij}(\mathbf{x}, \mathbf{y}, t_1, t_2)$ constructed in the same way as \mathcal{B}_{ij} .

For a particular model of turbulence (short-correlated random flow), Kazantsev (1967), and simultaneously Kraichnan and Nagarajan (1967) for a slightly different model, obtained a governing equation known now as the Kazantsev equation. In particular Kazantsev (1967) assumed $\mathcal{V}_{ij}(\mathbf{x}, \mathbf{y}, t_1, t_2) = \bar{\mathcal{V}}_{ij}(\mathbf{x}, \mathbf{y}) \delta(t_1 - t_2)$, and derived an evolution equation for the magnetic field correlation tensor calculated at two simultaneous instants $\mathcal{B}_{ij}(\mathbf{x}, \mathbf{y}, t) = \mathcal{B}_{ij}(\mathbf{x}, \mathbf{y}, t, t)$, with $t_1 = t_2 = t$. This reads

$$\frac{\partial \mathcal{B}_{ij}}{\partial t} = \hat{L}_{ijkm} \mathcal{B}_{km} \quad (12)$$

where \hat{L}_{ijkm} is a second-order differential operator with coefficients depending on $\bar{\mathcal{V}}_{ij}$, its spatial derivatives and coefficient of magnetic diffusion η . In some sense, the Kazantsev equation is similar to the famous Steenbeck-Krause-Rädler α effect equation in mean-field electrodynamics. In practice however the latter equation provided much more astronomically fruitful results than the first one. The reason is presumably two-fold. First of all, the Kazantsev equation requires more algebra for its solution than the mean-field equations. We only take here some new points isolated recently in this bulky algebra and refer to a detailed review given by Zeldovich et al. (1990). The other reason is that the physical interpretation of solutions of Eq. (12) is more delicate than that for the mean-field equation. This is the main issue presented in following sections.

Original insight which lead Kazantsev to Eq. (12) required some mathematics from quantum field theory that can hardly be considered ‘user friendly’ for a person with an ordinary MHD background. A more familiar approach, which is however rather bulky, can be found elsewhere (Zeldovich et al. 1990; Subramanian 1997; Brandenburg and Subramanian 2005a). The particular form of the Kazantsev equation (12) is associated with a specific model of turbulence assumed, in particular the assumption of δ -correlated (in time) velocity fluctuations. This model is quite restrictive and does not allow one to represent adequately some basic properties of the Kolmogorov cascade. Various attempts to derive this equations for more realistic models were undertaken (see, e.g., Kleorin et al. 2002). For example, incorporating a finite

correlation time results in quite complicated albeit beautiful mathematics and gives rise to integral equations. As far as it is known however the results are more or less the same if just applied to Eq. (12) with \bar{V}_{ij} taken from a suitable model of turbulence ignoring the fact that this very model is incompatible with the derivation of Eq. (12).

A reasonable way to simplify Eq. (12) to a useful level is to consider statistically homogeneous, isotropic and mirror-symmetric turbulence and look for solutions having the same symmetry. This means that we exploit a velocity correlation tensor of the form

$$\bar{V}_{ij} = A(r)r_i r_j + B(r)\delta_{ij} \quad (13)$$

($\mathbf{r} = \mathbf{y} - \mathbf{x}$) and look for the magnetic field correlation tensor in a similar form. The incompressibility condition means that the functions A and B depend on a single function, say, $F(r)$ while the solenoidality condition of the magnetic field means that \mathcal{B}_{ij} depends on a single function, say, $W(r, t)$. Then Eq. (12) can be reduced to a single second-order ordinary differential equation for a single function which depends on W with coefficients depending on F . In fact it is the equation which was obtained by Kazantsev (1967). The algebra here remains quite bulky and we avoid to present it here in detail; see, for example, the detailed discussions in Zeldovich et al. (1990) and Brandenburg and Subramanian (2005a).

There is no problem to solve the Kazantsev equation in the homogeneous and isotropic case for a particular choice of F numerically or by analytical approximations. In fact the Kazantsev equation can be reformulated as a Schrödinger type equation for a particle with variable mass $m(r)$ in a potential $U(r)$ (both of which depend on $F(r)$), whose bound states correspond to exponentially growing $W(r, t)$. It is possible to develop a WKB-like method for an approximate solution in the limit of large magnetic Reynolds numbers Re_M ($\sim \eta^{-1}$).

A general result following from these solutions can be summarized as follows. For a sufficiently large Re_M , the magnetic field correlation tensor (i.e. W) grows exponentially with a growth rate γ_2 which is determined by l/v where l is the turbulence correlation time and v is its rms velocity. The critical magnetic Reynolds number is of order $R_{m,\text{crit}} \approx 10^2$, with $R_{m,\text{crit}} = 26$ in the most simple example with $F = \exp -(r/l)^2$. For this illustrative example, function W which determines the magnetic field correlation properties has quite a complicated form which contains spatial scales from l up to $l\text{Re}_M^{-1/2}$.

A plausible scenario for the nonlinear saturation of the growth of the magnetic field correlation tensor governing the Kazantsev equation was suggested by Subramanian (1999). The main idea here is that nonlinearity results in an effective suppression of Re_M up to $R_{m,\text{crit}}$. It is quite straightforward to consider Kazantsev equation for homogeneous, isotropic and mirror-asymmetric turbulence and to combine concepts of the second-order correlation tensor with the mean-field approach (Subramanian 1999; Gabov and Sokoloff 2004). Interestingly, the Kazantsev equation in the presence of kinetic helicity, can be reformulated into a tunnelling type quantum mechanical problem, where by the bound states of the small scale dynamo can ‘tunnel’ to develop long range correlations (Subramanian 1999; Brandenburg and Subramanian 2000; Boldyrev et al. 2005). It is also possible to solve the Kazantsev equation for locally homogeneous and isotropic turbulence in a finite body of size $L \gg l$ (Maslova et al. 1987; Belyanin et al. 1993).

3.2 Random magnetic fields in cosmology

The description of a random magnetic field by a second-order correlation function is widely exploited in cosmology. To be specific, Chernin (1966) considered at first a cosmological model with a random magnetic field and discussed cosmological evolution of its magnetic energy. We have to stress however that the concepts of statistical hydrodynamics, which are a mathematical basis for the Kazantsev approach, need some modification to be applicable for curved spaces of General Relativity. The point is that Eq. (11) considers the product of two vectors applied at different spatial points while such option is absent in Riemannian geometry. We have to consider a geodesic line connecting points \boldsymbol{x} and \boldsymbol{y} , transport a field from the second point to the first one and consider product of the two fields applied at one spatial point. This recipe presumes that a geodesic line which leaves a point \boldsymbol{x} does no longer cross other geodesic lines which leave this point. In other words this means that geodesic lines do not contain conjugated points and the space-time has no gravitational lenses. If they do exist we have to elaborate somehow the concept of the correlation tensor and no general recommendations are suggested until now.

Then statistical homogeneity, isotropy and mirror symmetry in a curved spatial section of a Friedmann cosmological model reads

$$\mathcal{B}^{ij} = C(r)n^i n^j + D(r)g^{ij}, \quad (14)$$

i.e. we have to distinguish upper and lower indices and use tangent vector n^i of the geodesic line connecting \boldsymbol{x} and \boldsymbol{y} instead of the vector \boldsymbol{r} which do not exist in a curved space. The other point is that one deals with a curved space formulation of solenoidality condition to reduce C and D with one one function. Inspired by earlier work of Garcia de Andrade (2010), Rubashny and Sokoloff (2010) performed a corresponding analysis to show that for the Lobachevsky space with negative curvature,

$$C = -R \frac{\text{th} \frac{r}{R}}{2} F', \quad D = F + R \frac{\text{th} \frac{r}{R}}{2} F'. \quad (15)$$

where R is the curvature radius of the spatial section and r is distance between \boldsymbol{x} and \boldsymbol{y} . It is instructive to compare this representation with that for Euclidean space

$$C = -\frac{r}{2} F', \quad D = F + \frac{r}{2} F'. \quad (16)$$

Because $\text{th} \frac{r}{R}$ has a finite limit at $r/R \rightarrow \infty$, correlations decay slightly slower for the Lobachevsky space rather in the Euclidean space (of course F is the same in both cases). More significantly, however, the volume of a sphere with radius r grows exponentially in the Lobachevsky space and not as a power law like in Euclidean space. It means that F has to decay much faster in Lobachevsky space than in Euclidean space to get convergence of various spatial means which are based on the correlation tensor.

For a spherical space (closed cosmological model) one obtains

$$C = -R \frac{\text{tg} \frac{r}{R}}{2} F', \quad D = F + R \frac{\text{tg} \frac{r}{R}}{2} F'. \quad (17)$$

This representation gives $C(\pi R) = 0$, i.e., C vanishes if \boldsymbol{y} is just the opposite point to \boldsymbol{x} . This looks reasonable because n^i is not determined uniquely for the opposite points. $\text{tg} \frac{r}{R}$ diverges for $r = \pi R/2$ so the finiteness of correlations means that $F'(\frac{\pi R}{2}) = 0$.

This condition is specific for spherical geometry and has no direct analogues for the Euclidean one. Remarkably, a closed universe admits another homogeneous and isotropic topological structure of spatial section, namely an elliptical space which is twice smaller than the spherical one. Instead of the above condition we find here $F''(\pi R/2) = 0$. Moreover, an elliptical space does not admit orientation, so one cannot distinguish between left- and right-hand coordinate system there. It means that quantities such as helicities, α effect and other pseudo-scalar quantities cannot be introduced there. Such topological constrains on the magnetic field correlation properties look rather strange. Fortunately they do not affect substantially physically interesting conclusions because the correlation length l is usually much smaller than the curvature radius R . The problem however is that both quantities as well as the horizon radius vary strongly during the course of cosmological evolution that is given l being negligible in the present day cosmological scale might be very large in scales of the Early Universe. A more severe problem arises if we are going to consider a homogeneous and isotropic ensemble of random gravitational waves (Ivanova and Sokoloff 2008), which are often discussed in cosmological context.

3.3 Higher statistical moments and intermittency

To get more detailed information concerning a dynamo-generated small-scale magnetic field, it is useful to consider higher statistical moments which are introduced as *ensemble* averages of a product of p magnetic field vectors (p is the order of statistical moment). Following the Kazantsev approach one can obtain the governing equations for these quantities and demonstrate that the moments grow provided Re_M is high enough (see, e.g., Kleorin et al. 2002). Of course, the algebra becomes more bulky as m increases. The problem is that the higher moments grow faster than the lower ones in the sense that

$$\gamma_2/2 < \gamma_4/4 < \gamma_6/6 \dots \quad (18)$$

Of course, this fact can be supported by a direct calculation. However, it is much more instructive to demonstrate the phenomenon at a qualitative level (e.g. Molchanov et al. 1988). Let us consider a flow with a memory time τ so the magnetic field $\mathbf{B}(n\tau)$ at instant $n\tau$ can be considered to be developed from the initial field $\mathbf{B}(0)$ which is affected by n independent random transport operators \hat{T}_i

$$\mathbf{B}(n\tau) = \hat{T}_n \hat{T}_{n-1} \dots T_1 \mathbf{B}(0). \quad (19)$$

As a matter of fact, progressive growth of higher statistical moments in Eq. (18) does not depend critically on the fine structure of operators \hat{T}_i so we can illustrate the phenomenon by considering the simplest operators \hat{T}_i , i.e. just independent random numbers T_i .

For the sake of definiteness, let $\ln T_i$ have Gaussian distribution with zero mean and standard deviation σ . Then

$$T = T_n T_{n-1} \dots T_1 \quad (20)$$

is a log-normal random quantity and $\ln T$ has zero mean and standard deviation $\sqrt{n}\sigma = \sigma\sqrt{t/\tau}$. A straightforward calculation shows that

$$\langle T^p \rangle = \exp(\sigma^2 p^2 t / 2\tau), \quad (21)$$

so the normalized growth rates of the moments $\gamma_p/p = \sigma^2 p/2\tau$ grow linearly with the degree p of statistical moment. The other point is that the growth is determined not by a typical value of T_i which is of order σ , but by strong deviations which are of order $\sigma\sqrt{tp/\tau}$. The probability density of a Gaussian quantity to achieve the level $\sigma\sqrt{tp/\tau}$ is of order $\exp(-tp/2\tau)$ so the size N of a statistical ensemble should be as large as $N^*(t) = \exp(tp/2\tau)$ to include such rare events.

Note that the above analysis presumes that the statistical ensemble is infinitely large. If the ensemble is only large but finite its size N should exceed a critical value $N^*(t)$ which grows in time exponentially. For large t we obtain $N < N^*(t)$ and the above estimates becomes inapplicable.

If we consider a medium of independent cells of size l renovating after a memory time τ , then the critical size of the system which allows one to recognize the growth governed by Eq. (21) is given by

$$L^*(t) = lN^{1/3} = l \exp(tp/6\tau). \quad (22)$$

This means that the behavior of the statistical moment of the order p is determined by very rare cells and Eq. (22) gives an estimate for the distance to the nearest cell which determines the moment at a given point. The phenomenon of a random field whose properties are determined by rare and remote events is known as intermittency. The wording comes from medicine and means a state when a person is near death, but his/her heart still works from time to time. These rare events of the heart activity determine the fact that the person is still alive.

Note that if we calculated a PDF of T based on a limited sample with $N < N^*(t)$ it is practically impossible to recognize the existence of the above mentioned rare events which do not contribute to the PDF calculated. Of course, the importance of the result depends on how large t should be to make the intermittency recognizable and how large the corresponding value N^* is in comparison with N typical of celestial bodies.

It is natural to address this point based on a simple physical example rather than just a product of random operators. A simple example of this kind accessible for simple numerics has been suggested by Zeldovich (1964) in a cosmological context. Let a remote object have a (small) angular size θ , let x be the distance to the object and $y = \theta x$ its linear size. $y(x)$ is known in the Riemannian geometry as Jacobi field and is governed by the so-called Jacobi equation

$$y'' + Ky = 0, \quad (23)$$

where a prime means the derivative taken with respect to x and K is the spatial (sectional) curvature. Zeldovich (1964) recognized the importance of density and then curvature fluctuations on the evolution of y along the line of sight. In other words, we consider K as a random, say, Gaussian quantity.

It is quite easy to simulate many independent solutions of Eq. (23) and determine experimentally how large $N^*(t)$ is. It appears (Artyushkova and Sokoloff 2005) that one needs $N \approx 5 \times 10^5 \dots 10^6$ to recognize the difference between $\gamma_2/2$ and $\gamma_4/4$ for $t \approx 10^2$. Of course, a simulation of 10^6 independent 3D cells for a hundred turnover times becomes prohibitive given the purely computational problems, in addition to the problems associated with the further data processing of the results. On the other hand, the number of independent turbulent cells in a typical galaxy is of order of 10^6 so the effects of intermittency can contribute in mean quantities of interest for

galactic dynamos. In practice however the difference between $\gamma_2/2$ and $\gamma_4/4$ is for the intermittent fields, as far as it is known, not very large.

The other point here is that the growing magnetic field becomes sooner or later dynamically important. Of course, it is important to know which happens first, whether the field becomes dynamically important first or whether the size of the domain becomes too small to contain the intermittent structure? Unfortunately, the abilities of simple models like Eq. (23) to reproduce the stage of nonlinear dynamo saturation are limited. A numerical experiment with a simple model shows that the number N required to reproduce the behavior of higher statistical moments declines strongly when the solution becomes dynamically important such that exponential growth of statistical moments saturates.

Yet another point which can be recognized from the experiences with simple models is that ensemble averaging is not the only option to describe the behavior of the growing solution. Lamburt et al. (2003) demonstrated that the quantity

$$\frac{\ln |y|}{t} \rightarrow \gamma > 0 \quad (\text{for } t \rightarrow \infty) \quad (24)$$

for almost all realizations (with probability 1, or “almost sure” in the wording of probability theory) where no averaging is taken at all. Quantities such as γ are known as self-averaging quantities and γ in particular is known as Lyapunov exponent. The phenomenon becomes clearer if one introduces a 2D row-vector (y, y') and rewrites Eq. (23) as a vectorial equation

$$z' = z\hat{A}, \quad (25)$$

where \hat{A} is a random matrix process with vanishing trace (i.e. $\text{Tr } \hat{A} = 0$). Then the evolution of z from an initial condition z_0 can be represented as a product of independent random unimodular matrices $B_i = \exp(\hat{A}_i\tau)$, $\det B_i = 1$, where \hat{A}_i is a realization at a given interval of renovation of the random matrix process \hat{A} .

The product of independent random matrices is quite well investigated in probability theory (so-called Furstenberg theory). Zeldovich et al. (1984) stressed the importance of this theory for small-scale dynamos (here the elements of \hat{A} are $\partial v_i/\partial x_j$). Molchanov et al. (1984) argue that magnetic field generated by a small-scale dynamo grows such that

$$\frac{\ln |\mathbf{B}|(\mathbf{x}, t)}{t} \rightarrow \gamma > 0 \quad \text{for } t \rightarrow \infty, \quad (26)$$

where γ is a positive constant. A numerical experiment for the Jacobi equation supports this interpretation and shows that t should be of the order of a hundred memory times to get this behavior (Artyushkova and Sokoloff 2005). The PDF of the dynamo-excited magnetic field is investigated by Chertkov et al. (1999).

Unfortunately, this approach of simple models cannot mimic the α effect. The point is that one cannot produce a pseudoscalar quantity α based on correlations of A_{ij} and A_{mn} and a Levi-Civita tensor ϵ_{pqr} .

Generally speaking, the analytical results discussed above show that detailed direct numerical simulations of small-scale dynamos at the kinematic stage can be nontrivial to interpret due to the rapidly growing intermittency. Fortunately, the magnetic field becomes dynamically important quite rapidly (at least at small scales), so the dynamo becomes nonlinear and mathematical distinctions between properties of various statistical moments become less and less important. Artyushkova and Sokoloff (2005) investigated several simple models how catastrophic intermittency typical of the kinematic stage gradually evaporate when nonlinear effects become important. Presumably,

something like that happens for the much more complicated full small-scale dynamo equations.

3.4 Small-scale magnetic field and shell models

The Kazantsev model is developed for the kinematic or weakly nonlinear stage of the dynamo and its ability to describe the strongly nonlinear stage of a dynamo is obviously quite limited. However, it remains useful to have a simple model of strongly nonlinear dynamos in terms of ordinary (instead of partial) differential equations. An option of this kind is given by so-called shell models of MHD-turbulence.

The starting point of the shell model approach is to note that for random fields and flows, one can hardly reproduce in a numerical simulation the actual realization of the random field which are obtained in a given celestial body. In practice we are interested in some spectral properties of the field of interest. If we can get such properties without solving the full set of equations, we would be happy with such a result.

Shell models are designed to describe the cascade process over a large range of scales (wavenumbers) by a chain of variables $u_n(t)$, $b_n(t)$, each of them characterizing velocity or magnetic field oscillations with wavenumbers k in the range from $k_n = k_0 \lambda^n$ to k_{n+1} i.e., a shell of wavenumbers. The parameter λ characterizes the ratio of two adjacent scales (the width of the shell) and usually $\lambda \leq 2$. The model includes a corresponding set of ordinary differential equations, which should reproduce the basic properties of the equation of motion. In particular, the model has to reproduce the type of nonlinearity of the primitive equations and to retain the same integrals of motion in the dissipationless limit. Let us note that shell models can possess positively defined integrals of motion (energy, enstrophy in two-dimensional turbulence, and the square of magnetic potential in 2D MHD-turbulence), as well as quadratic integrals with an arbitrary sign (the integrals of this kind are usually called ‘helicities’). The signs of the helicities are defined by the balance between the contributions of odd and even shells to corresponding quantity.

The shell models were suggested by Kolmogorov’s school to describe the spectral energy transfer (Gledzer 1973; Desnianskii and Novikov 1974). After numerous refinements they became an effective tool for description of the spectral properties of the small-scale turbulence (see for review Bohr et al. 1998). The shell models for MHD turbulence were introduced by Frick (1984), Gloaguen et al. (1985), Brandenburg et al. (1996), and Frick and Sokoloff (1998). This approach reveals many intrinsic features of small-scale dynamo action in fully developed turbulence of conducting fluids (for review see Biferale 2003). In particular, the shell model suggested by Frick and Sokoloff (1998) gives a fast growth of small-scale magnetic fields (on the timescale l/v) and its saturation at the equipartition level as well as non-Gaussian (similar to lognormal) PDF for small-scale magnetic field in the saturated state. In some cases shell models give a hint concerning dynamo action in the parametric domain inaccessible to direct numerical simulations. In particular, Stepanov and Plunian (2006) and Frick et al. (2006) argue, based on simulations of MHD-shell models, that the critical magnetic Reynolds number for small-scale dynamo action remains moderate $R_{m,crit} \approx 80$ in the case of low Prandtl numbers. This is also confirmed by the simulations discussed in Section 2.2. General speaking, shell models seem to provide an effective way to investigate small-scale dynamos.

It may be possible to combine shell models as a tool to describe small-scale variables in a dynamo with grid or spectral methods for large-scale variables in mean-field equations. However only the first steps in this direction have been made until now (Frick et al. 2002, 2006; Nigro and Veltri 2011).

3.5 Dynamical chaos and small-scale dynamo

One more point of comparison between numerical and analytical approaches to the small-scale dynamos is as follows. The Kazantsev model and its related investigations consider turbulence as a truly random field and apply concepts of probability theory in full extent. In contrast, direct numerical simulations and shell models consider turbulence as a chaotic behavior of solutions for deterministic equations of motion. It is quite risky to insist *a priori* that dynamical chaos reproduces all properties of random flows required for analytical approaches. It is even less obvious that interstellar turbulence driven by supernova explosions (e.g. Korpi et al. 1999; Gressel et al. 2008) provides a truly random velocity field. On the other hand, dynamo models based on steady flows with stochastic flow lines such as ABC flows excite magnetic fields which look rather different from the field discussed for turbulent dynamos. Zeldovich (see Zeldovich et al. 1983) suggested that dynamo action in nonstationary flows (say, when parameters A , B and C in the ABC flow fluctuate in time) becomes much more similar to the dynamo action in random flows than dynamos in stationary flows. Recent work of Kleorin et al. (2009) supports this idea and demonstrates that in a fluctuating ABC flow, a large-scale magnetic field can indeed grow in a way similar to what is supposed to grow in a random mirror-asymmetric (helical) turbulent flow.

4 Conclusions

In this review we have discussed our current understanding of both large-scale and small-scale dynamos that are relevant in astrophysics. In particular, we have illustrated differences and similarities between them and have compared them in terms of the energy spectra with the corresponding cases at low magnetic Prandtl numbers. We have also briefly highlighted the resistively slow saturation phenomenon as well as catastrophic quenching of helicity-driven large-scale dynamos. Finally, we have discussed new issues in connection with small-scale dynamos and their intermittency.

Relative to earlier reviews (e.g. Brandenburg and Subramanian 2005a) there have been some unexpected advances regarding the nature of magnetic helicity fluxes and direct observational evidence for magnetic helicity in the solar wind. Another completely unexpected development concerns the numerical detection of the negative effective magnetic pressure instability in simulations of strongly stratified turbulence. It is expected that these developments will contribute to an improved understanding of the magnetic field generation in astrophysical bodies. On the technical side, Brandenburg and Subramanian (2005a) discussed just the basics of the test-field method, but now this technique has provided significant insights into issues such as non-locality in space and time, as well as the nonlinear quenching of dynamo coefficients.

In this review we have barely touched upon applications to actual astrophysical bodies. In fact, a lot of progress has been made by trying to model the Sun. Direct nu-

merical simulations of convection in spherical shells has shown signs of cyclic large-scale fields (Brown et al. 2010, 2011; Käpylä et al. 2010; Ghizaru et al. 2010; Racine et al. 2011), but only for systems that are rotating at least 3 times faster than the Sun; see Brown et al. (2011) for simulations with otherwise realistic solar parameters. Similar results have also been obtained for local simulations of the galactic dynamo, which only appears to be excited when the rotation speed is artificially enhanced (Gressel et al. 2008). This might well indicate that one is on the right track, but that the turbulence present in the system is exerting too much effective diffusion owing to it being dominated by rather large eddies. It is conceivable that in reality the turbulent eddies would be smaller, lowering thereby the effective turbulent diffusion, which can at the moment (with the larger eddies) only be emulated by adopting faster rotation. Similar results have recently also been seen in models of the negative effective magnetic pressure instability, where direct numerical simulations showed the development of the instability only when there were enough turbulent eddies in the domain and thereby the turbulent diffusivity sufficiently small on that scale; see Brandenburg et al. (2011) and, in particular, Figure 17 of Brandenburg et al. (2012). Thus, much has been learned about turbulent dynamos and their relevance for astrophysical systems but as usual, much remains to be elucidated.

Acknowledgements We thank Andre Balogh for providing an inspiring atmosphere at the International Space Science Institute in Bern in 2010, which has led to new collaborations and scientific progress. Computing resources were provided by the Swedish National Allocations Committee at the Center for Parallel Computers at the Royal Institute of Technology in Stockholm and the High Performance Computing Center North in Umeå. This work was supported in part by the European Research Council under the AstroDyn Research Project No. 227952 and the Swedish Research Council under the project grant 621-2011-5076.

References

- M.E. Artyushkova, D.D. Sokoloff, Numerical modelling of the solutions of the Jacobi equation on a geodesic with random curvature, *Astron. Rep.* **49**, 520-525 (2005)
- G.K. Batchelor, On the spontaneous magnetic field in a conducting liquid in turbulent motion, *Proc. Roy. Soc. Lond.* **A201**, 405-416 (1950)
- R. Beck, A. Brandenburg, D. Moss, A. Shukurov, D. Sokoloff, Galactic Magnetism: Recent Developments and Perspectives, *Ann. Rev. Astron. Astrophys.* **34**, 155-206 (1996)
- M.P. Belyanin, D. Sokoloff, A. Shukurov, Simple models of nonlinear fluctuation dynamo, *Geophys. Astrophys. Fluid Dynam.* **68**, 237-261 (1993)
- E.E. Benevolenskaya, J.T. Hoeksema, A.G. Kosovichev, P.H. Scherrer, The interaction of new and old magnetic fluxes at the beginning of solar cycle 23, *Astrophys. J.* **517**, L163-L166 (1999)
- L. Biermann, A. Schlüter, Cosmic radiation and cosmic magnetic fields. II. Origin of cosmic magnetic fields, *Phys. Rev.* **82**, 863-868 (1951)
- L. Biferale, Role of inviscid invariants in shell models of turbulence, *Ann. Rev. Fluid Dyn.* **35**, 441-6122 (2003)
- E.G. Blackman, G.B. Field, Constraints on the magnitude of α in dynamo theory, *Astrophys. J.* **534**, 984-988 (2000a)
- E.G. Blackman, G.B. Field, Coronal activity from dynamos in astrophysical rotators, *Monthly Notices Roy. Astron. Soc.* **318**, 724-724 (2000b)
- E.G. Blackman, A. Brandenburg, Dynamic nonlinearity in large scale dynamos with shear, *Astrophys. J.* **579**, 359-373 (2002)
- E.G. Blackman, A. Brandenburg, Doubly helical coronal ejections from dynamos and their role in sustaining the solar cycle, *Astrophys. J. Letters* **584**, L99-L102 (2003)
- E.G. Blackman, G.B. Field, New dynamical mean-field dynamo theory and closure approach, *Phys. Rev. Letters* **89**, 265007 (2002)

-
- T. Bohr, M.H. Jensen, G. Paladin, A. Vulpiani Dynamical Systems Approach to Turbulence. Cambridge: Cambridge University Press (1998)
- S. Boldyrev, F. Cattaneo, R. Rosner, *Phys. Rev. Letters* **255001**, Magnetic-field generation in helical turbulence (2005)
- S. Boldyrev, J.C. Perez, J.E. Borovsky, J.J. Podesta, Spectral Scaling Laws in Magnetohydrodynamic Turbulence Simulations and in the Solar Wind, *Astrophys. J.* **741**, L19 (2011)
- A. Brandenburg, The inverse cascade and nonlinear alpha-effect in simulations of isotropic helical hydromagnetic turbulence, *Astrophys. J.* **550**, 824-840 (2001)
- A. Brandenburg, The case for a distributed solar dynamo shaped by near-surface shear, *Astrophys. J.* **625**, 539-547 (2005a)
- A. Brandenburg, Turbulence and its parameterization in accretion discs, *Astron. Nachr.* **326**, 787-797 (2005b)
- A. Brandenburg, Large-scale dynamos at low magnetic Prandtl numbers, *Astrophys. J.* **697**, 1206-1213 (2009)
- A. Brandenburg, Nonlinear small-scale dynamos at low magnetic Prandtl numbers, *Astrophys. J.* **741**, 92 (2011a)
- A. Brandenburg, Chandrasekhar-Kendall functions in astrophysical dynamos, *Pramana J. Phys.* **77**, 67-76 (2011b)
- A. Brandenburg, K. Subramanian, Large scale dynamos with ambipolar diffusion nonlinearity, *Astron. Astrophys.* **361**, L33-L36 (2000)
- A. Brandenburg, K. Subramanian, Astrophysical magnetic fields and nonlinear dynamo theory, *Phys. Rep.* **417**, 1-209 (2005a)
- A. Brandenburg, K. Subramanian, Strong mean field dynamos require supercritical helicity fluxes, *Astron. Nachr.* **326**, 400-408 (2005b)
- A. Brandenburg, S. Candelaresi, P. Chatterjee, Small-scale magnetic helicity losses from a mean-field dynamo, *Monthly Notices Roy. Astron. Soc.* **398**, 1414-1422 (2009)
- A. Brandenburg, W. Dobler, K. Subramanian, Magnetic helicity in stellar dynamos: new numerical experiments, *Astron. Nachr.* **323**, 99-122 (2002)
- A. Brandenburg, K. Enqvist, P. Olesen, Large-scale magnetic fields from hydromagnetic turbulence in the very early universe, *Phys. Rev. D* **54**, 1291-1300 (1996)
- A. Brandenburg, P. Käpylä, A. Mohammed, A., Non-Fickian diffusion and tau-approximation from numerical turbulence, *Phys. Fluids* **16**, 1020-1027 (2004)
- A. Brandenburg, K. Kemel, N. Kleeorin, D. Mitra, I. Rogachevskii, Detection of negative effective magnetic pressure instability in turbulence simulations, *Astrophys. J.* **740**, L50 (2011)
- A. Brandenburg, K. Kemel, N. Kleeorin, I. Rogachevskii, Effect of stratified turbulence on magnetic flux concentrations, *Astrophys. J.*, arXiv:1005.5700 (2012)
- A. Brandenburg, N. Kleeorin, I. Rogachevskii, Large-scale magnetic flux concentrations from turbulent stresses, *Astron. Nachr.* **331**, 5-13 (2010)
- A. Brandenburg, D. Moss, A.M. Soward, New results for the Herzenberg dynamo: steady and oscillatory solutions, *Proc. Roy. Soc. A* **454**, 1283-1300 (1998)
- A. Brandenburg, K.-H. Rädler, M. Rheinhardt, P.J. Käpylä, Magnetic diffusivity tensor and dynamo effects in rotating and shearing turbulence, *Astrophys. J.* **676**, 740-751 (2008)
- A. Brandenburg, K.-H. Rädler, M. Rheinhardt, K. Subramanian, Magnetic quenching of alpha and diffusivity tensors in helical turbulence, *Astrophys. J.* **676**, 740-L52 (2008)
- A. Brandenburg, K.-H. Rädler, M. Schinner, Scale dependence of alpha effect and turbulent diffusivity, *Astron. Astrophys.* **482**, 739-746 (2008)
- A. Brandenburg, K. Subramanian, A. Balogh, M.L. Goldstein, Scale-dependence of magnetic helicity in the solar wind, *Astrophys. J.* **734**, 9 (2011)
- B.P. Brown, M.K. Browning, A.S. Brun, M.S. Miesch, J. Toomre, Persistent magnetic wreaths in a rapidly rotating Sun, *Astrophys. J.* **711**, 424-438 (2010)
- B.P. Brown, M.S. Miesch, M.K. Browning, A.S. Brun, J. Toomre, Magnetic Cycles in a Convective Dynamo Simulation of a Young Solar-type Star, *Astrophys. J.* **731**, 69 (2011)
- S. Candelaresi, A. Hubbard, A. Brandenburg, D. Mitra, Magnetic helicity transport in the advective gauge family, *Phys. Plasmas* **18**, 012903 (2011)
- F. Cattaneo, S.M. Tobias, Dynamo properties of the turbulent velocity field of a saturated dynamo, *J. Fluid Mech.* **621**, 205-214 (2009)
- L. Chamandy, K. Subramanian, A. Shukurov, Galactic spirals and dynamo action: Slaved non-axisymmetric modes (in preparation).

- P. Chatterjee, G. Guerrero, A. Brandenburg, Magnetic helicity fluxes in interface and flux transport dynamos, *Astron. Astrophys.* **525**, A5 (2011)
- A.D. Chernin, A Cosmological Model with a Disordered Magnetic Field, *Astron. Zh.* **43**, 797-801 (1966)
- M. Chertkov, G. Falkovich, I. Kolokolov, M. Vergassola, Small-Scale Turbulent Dynamo, *Phys. Rev. Letters* **83**, 4065-4068 (1999)
- J. Cho, D. Ryu, Characteristic lengths of magnetic field in magnetohydrodynamic turbulence, *Astrophys. J.* **705**, L90-L94 (2009)
- A.R. Choudhuri, M. Schüssler, M. Dikpati, The solar dynamo with meridional circulation, *Astron. Astrophys.* **303**, L29-L32 (1995)
- A. Courvoisier, D.W. Hughes, S.M. Tobias, α -effect in a family of chaotic flows, *Phys. Rev. Letters* **96**, 034503 (2006)
- V.N. Desnianskii, E.A. Novikov, Simulation of cascade processes in turbulent flows, *Prikl. Mat. Mekh.* **38**, 507-512 (1974)
- M. Dikpati, P. Charbonneau, A Babcock-Leighton flux transport dynamo with solar-like differential rotation, *Astrophys. J.* **518**, 508-520 (1999)
- P. Dittrich, S.A. Molchanov, D.D., Sokolov, A.A. Ruzmaikin, Mean magnetic field in renovating random flow, *Astron. Nachr.* **305**, 119-125 (1984)
- W.M. Elsasser, Hydromagnetic Dynamo Theory, *Rev. Mod. Phys.* **28**, 135-163 (1956)
- G.L. Eyink, Stochastic flux freezing and magnetic dynamo, *Phys. Rev.* **83**, 056405 (2011)
- S. Fedotov, I. Bashkirtseva, L. Ryashko, Memory effects in a turbulent dynamo: generation and propagation of a large-scale magnetic field, *Phys. Rev.* **73**, 066307 (2006)
- G.B. Field, E.G. Blackman, Dynamical quenching of the α^2 dynamo, *Astrophys. J.* **572**, 685-692 (2002)
- P.G. Frick, Two-dimensional MHD turbulence. Hierarchical Model, *Magnetohydrodynamics* **20**, 262-267 (1984)
- P. Frick, D. Sokoloff, Cascade and dynamo action in a shell model of magnetohydrodynamic turbulence, *Phys. Rev. E* **57**, 4155-4164 (1998)
- P. Frick, M. Reshetnyak, D. Sokoloff, Combined grid-shell approach for convection in a rotating spherical layer, *Europhys. Lett.* **59**, 212-217 (2002)
- P. Frick, R. Stepanov, D. Sokoloff, Large- and small-scale interactions and quenching in an 2-dynamo, *Phys. Rev.* **74**, 066310 (2006)
- U. Frisch, A. Pouquet, J. Léorat, A. Mazure, Possibility of an inverse cascade of magnetic helicity in hydrodynamic turbulence, *J. Fluid Mech.* **68**, 769-778 (1975)
- U. Frisch, Z.-S. She, P.L. Sulem, Large-scale flow driven by the anisotropic kinetic alpha effect, *Physica* **28D**, 382-392 (1987)
- S.A. Gabov, D.D. Sokoloff, Current helicity and the small-scale dynamo, *Astron. Rep.* **48**, 949-953 (2004)
- D. Galloway, U. Frisch, Dynamo action in a family of flows with chaotic streamlines, *Geophys. Astrophys. Fluid Dynam.* **36**, 53-84 (1986)
- D.J. Galloway, M.R.E. Proctor, Numerical calculations of fast dynamos in smooth velocity fields with realistic diffusion, *Nature* **356**, 691-693 (1992)
- L.C. Garcia de Andrade, Primordial magnetic fields constrained from CMB anisotropies on dynamo cosmology, *Astrophys. Spa. Sci.* **330**, 347-351 (2010)
- M. Ghizaru, P. Charbonneau, P.K. Smolarkiewicz, Magnetic cycles in global large-eddy simulations of solar convection, *Astrophys. J.* **715**, L133-L137 (2010)
- A.D. Gilbert, B.J. Bayly, Magnetic field intermittency and fast dynamo action in random helical flows, *J. Fluid Mech.* **241**, 199-214 (1992)
- E.B. Gledzer, System of hydrodynamic type admitting two quadratic integrals of motion, *Sov. Phys. Dokl.* **18**, 216-221 (1973)
- C. Gloaguen, J. Léorat, A. Pouquet, R. Grappin, A scalar model for MHD turbulence, *Physica* **17D**, 154-182 (1985)
- G.S. Golitsyn, Fluctuations of the magnetic field and current density in a turbulent flow of a weakly conducting fluid, *Sov. Phys. Dokl.* **5**, 536-539 (1960)
- O. Gressel, D. Elstner, U. Ziegler, G. Rüdiger, Direct simulations of a supernova-driven galactic dynamo, *Astron. Astrophys.* **486**, L35-L38 (2008)
- A.V. Gruzinov, P.H. Diamond, Self-consistent theory of mean-field electrodynamics, *Phys. Rev. Letters* **72**, 1651-1653 (1994)
- N.E.L. Haugen, A. Brandenburg, W. Dobler, Is nonhelical hydromagnetic turbulence peaked at small scales?, *Astrophys. J.* **597**, L141-L144 (2003)

- N.E.L. Haugen, A. Brandenburg, W. Dobler, Simulations of nonhelical hydromagnetic turbulence, *Phys. Rev.* **70**, 016308 (2004)
- N.E.L. Haugen, A. Brandenburg, Hydrodynamic and hydromagnetic energy spectra from large eddy simulations, *Phys. Fluids* **18**, 075106 (2006)
- J.F. Hawley, C.F. Gammie, S.A. Balbus, Local three dimensional simulations of an accretion disk hydromagnetic dynamo, *Astrophys. J.* **440**, 742-763 (1995)
- T. Heinemann, J.C. McWilliams, A.A. Schekochihin, Magnetic-Field Generation by Randomly Forced Shearing Waves, *Phys. Rev. Letters* **107**, 255004 (2011)
- J. Herault, F. Rincon, C. Cossu, G. Lesur, G.I. Ogilvie, P.-Y. Longaretti, Periodic magnetorotational dynamo action as a prototype of nonlinear magnetic-field generation in shear flows, *Phys. Rev.* **84**, 036321 (2011)
- A. Herzenberg, Geomagnetic dynamos, *Proc. Roy. Soc. Lond.* **250A**, 543-583 (1958)
- A. Hubbard, A. Brandenburg, Memory effects in turbulent transport, *Astrophys. J.* **706**, 712-726 (2009)
- A. Hubbard, A. Brandenburg, Magnetic helicity fluxes in an α^2 dynamo embedded in a halo, *Geophys. Astrophys. Fluid Dynam.* **104**, 577-590 (2010)
- A. Hubbard, A. Brandenburg, Magnetic helicity flux in the presence of shear, *Astrophys. J.* **727**, 11 (2011)
- A. Hubbard, A. Brandenburg, Catastrophic quenching in $\alpha\Omega$ dynamos revisited, *Astrophys. J.* **748**, 51 (2012)
- A.B. Isakov, A.A. Schekochihin, S.C. Cowley, J.C. McWilliams, M.R.E. Proctor, Numerical demonstration of fluctuation dynamo at low magnetic Prandtl numbers, *Phys. Rev. Letters* **98**, 208501 (2007)
- E.V. Ivanova, D.D. Sokoloff, Statistically homogeneous and isotropic curvature fluctuations in general relativity, *Moscow Univ. Phys. Bull.* **63**, 109-111 (2008)
- P.J. Käpylä, M.J. Korpi, A. Brandenburg, Large-scale dynamos in turbulent convection with shear, *Astron. Astrophys.* **491**, 353-362 (2008)
- P.J. Käpylä, M.J. Korpi, A. Brandenburg, D. Mitra, R. Tavakol, Convective dynamos in spherical wedge geometry, *Astron. Nachr.* **331**, 73-81 (2010)
- A.P. Kazantsev, Enhancement of a magnetic field by a conducting fluid, *Sov. Phys. JETP* **53**, 1806-1809 (1967) [English translation, *JETP* 26, 1031 (1968).]
- K. Kemel, A. Brandenburg, N. Kleeorin, D. Mitra, I. Rogachevskii, Spontaneous formation of magnetic flux concentrations in stratified turbulence, *Solar Phys.*, DOI: 10.1007/s11207-012-9949-0 (2012)
- S. Kida, S. Yanase, J. Mizushima, Statistical properties of MHD turbulence and turbulent dynamo, *Phys. Fluids* **A 3**, 457-465 (1991)
- L.L. Kitchatinov, M.V. Mazur, Stability and equilibrium of emerged magnetic flux, *Solar Phys.* **191**, 325-340 (2000)
- N.I. Kleeorin, A.A. Ruzmaikin, Dynamics of the average turbulent helicity in a magnetic field, *Magnetohydrodynamics* **18**, 116-122 (1982) [Translation from *Magnitnaya Gidrodinamika*, 2, pp. 17-24 (1982).]
- N. Kleeorin, M. Mond, I. Rogachevskii, Magnetohydrodynamic instabilities in developed small-scale turbulence, *Phys. Fluids B* **5**, 4128-4134 (1993)
- N. Kleeorin, M. Mond, I. Rogachevskii, Magnetohydrodynamic turbulence in the solar convective zone as a source of oscillations and sunspots formation, *Astron. Astrophys.* **307**, 293-309 (1996)
- N. Kleeorin, I. Rogachevskii, Effective Ampère force in developed magnetohydrodynamic turbulence, *Phys. Rev. E* **50**, 2716-2730 (1994)
- N. Kleeorin, I. Rogachevskii, Mean-field dynamo in a turbulence with shear and kinetic helicity fluctuations, *Phys. Rev.* **77**, 036307 (2008)
- N.I. Kleeorin, I.V. Rogachevskii, A.A. Ruzmaikin, Negative magnetic pressure as a trigger of large-scale magnetic instability in the solar convective zone, *Sov. Astron. Letters* **15**, 274-277 (1989)
- N.I. Kleeorin, I.V. Rogachevskii, A.A. Ruzmaikin, Magnetic force reversal and instability in a plasma with advanced magnetohydrodynamic turbulence, *Sov. Phys. JETP* **70**, 878-883 (1990)
- N. Kleeorin, D. Moss, I. Rogachevskii, D. Sokoloff, Helicity balance and steady-state strength of the dynamo generated galactic magnetic field, *Astron. Astrophys.* **361**, L5-L8 (2000)
- N. Kleeorin, I. Rogachevskii, D. Sokoloff, Magnetic fluctuations with a zero mean field in a random fluid flow with a finite correlation time and a small magnetic diffusion, *Phys. Rev.*

- 65**, 036303 (2002)
- N. Kleorin, I. Rogachevskii, D. Sokoloff, D. Tomin, Mean-field dynamos in random Arnold-Beltrami-Childress and Roberts flows, *Phys. Rev.* **79**, 046302 (2009)
- M.J. Korpi, A. Brandenburg, A. Shukurov, I. Tuominen, and Å. Nordlund, A supernova regulated interstellar medium: simulations of the turbulent multiphase medium, *Astrophys. J.* **514**, L99-L102 (1999)
- R.H. Kraichnan, S. Nagarajan, Growth of turbulent magnetic fields, *Phys. Fluids* **10**, 859-870 (1967)
- F. Krause, K.-H. Rädler *Mean-field Magnetohydrodynamics and Dynamo Theory*. Oxford: Pergamon Press (1980)
- R.M. Kulsrud, S.W. Anderson, The spectrum of random magnetic fields in the mean field dynamo theory of the galactic magnetic field, *Astrophys. J.* **396**, 606-630 (1992)
- R.M. Kulsrud, E.G. Zweibel, On the origin of cosmic magnetic fields, *Rep. Progr. Phys.* **71**, 046901 (2008)
- V.G. Lamburt, V.N. Tutubalin, D.D. Sokoloff, Jacobi fields along a geodesic with random curvature, *Math. Not.* **74**, 393-400 (2003)
- T.B. Maslova, T.S. Shumkina, A.A. Ruzmaikin, D.D. Sokoloff, Self-excitation of fluctuation magnetic fields in a space contained by a random stream, *Sov. Phys. Dokl.* **32**, 520-521 (1987)
- M. Meneguzzi, U. Frisch, A. Pouquet, Helical and nonhelical turbulent dynamos, *Phys. Rev. Letters* **47**, 1060-1064 (1981)
- D. Mitra, A. Brandenburg, Scaling and intermittency in incoherent α -shear dynamo, *Monthly Notices Roy. Astron. Soc.* **420**, 2170-2177 (2012)
- D. Mitra, S. Candelaresi, P. Chatterjee, R. Tavakol, A. Brandenburg, Equatorial magnetic helicity flux in simulations with different gauges, *Astron. Nachr.* **331**, 130-135 (2010)
- H.K. Moffatt, The amplification of a weak applied magnetic field by turbulence in fluids of moderate conductivity, *J. Fluid Mech.* **11**, 625-635 (1961)
- H.K. Moffatt *Magnetic Field Generation in Electrically Conducting Fluids*. Cambridge: Cambridge Univ. Press (1978)
- S.A. Molchanov, A.A. Ruzmaikin, D.D. Sokoloff, A dynamo theorem, *Geophys. Astrophys. Fluid Dynam.* **30**, 241-259 (1984)
- S.A. Molchanov, A.A. Ruzmaikin, D.D. Sokoloff, Short-correlated random flow as a fast dynamo, *Sov. Phys. Dokl.* **32**, 569-570 (1988)
- D. Moss, On the generation of bisymmetric magnetic field structures in spiral galaxies by tidal interactions, *Monthly Notices Roy. Astron. Soc.* **275**, 191-194 (1995)
- D. Moss, R. Stepanov, T.G. Arshakian, R. Beck, M. Krause, D. Sokoloff, Multiscale magnetic fields in spiral galaxies: evolution and reversals, *Astron. Astrophys.* **537**, A68 (2012)
- G. Nigro, P. Veltri, A Study of the Dynamo Transition in a Self-consistent Nonlinear Dynamo Model, *Astrophys. J.* **740**, L37 (2011)
- E.N. Parker, Hydromagnetic dynamo models, *Astrophys. J.* **122**, 293-314 (1955)
- E.N. Parker, The dynamo dilemma, *Solar Phys.* **110**, 11-21 (1987)
- I.J. Parrish, E. Quataert, Nonlinear simulations of the heat-flux-driven buoyancy instability and its implications for galaxy clusters, *Astrophys. J.* **677**, L9-L12 (2008)
- I.J. Parrish, J.M. Stone, Nonlinear evolution of the magnetothermal instability in two dimensions, *Astrophys. J.* **633**, 334-348 (2005)
- I.J. Parrish, M. McCourt, E. Quataert, P. Sharma, The effects of anisotropic viscosity on turbulence and heat transport in the intracluster medium, *Monthly Notices Roy. Astron. Soc.* DOI:10.1111/j.1365-2966.2012.20650.x (2012)
- A. Pouquet, U. Frisch, J. Léorat, Strong MHD helical turbulence and the nonlinear dynamo effect, *J. Fluid Mech.* **77**, 321-354 (1976)
- M.R.E. Proctor, Effects of fluctuation on alpha-omega dynamo models, *Monthly Notices Roy. Astron. Soc.* **382**, L39-L42 (2007)
- É. Racine, P. Charbonneau, M. Ghizaru, A. Bouchat, P.K. Smolarkiewicz, On the Mode of Dynamo Action in a Global Large-eddy Simulation of Solar Convection, *Astrophys. J.* **735**, 46 (2011)
- K.-H. Rädler, N. Kleorin, I. Rogachevskii, The mean electromotive force for MHD turbulence: the case of a weak mean magnetic field and slow rotation, *Geophys. Astrophys. Fluid Dynam.* **97**, 249-274 (2003)
- K.-H. Rädler, R. Stepanov, Mean electromotive force due to turbulence of a conducting fluid in the presence of mean flow, *Phys. Rev.* **73**, 056311 (2006)

- M. Rheinhardt, A. Brandenburg, Test-field method for mean-field coefficients with MHD background, *Astron. Astrophys.* **520**, A28 (2010)
- M. Rheinhardt, A. Brandenburg, Modeling spatio-temporal nonlocality in mean-field dynamos, *Astron. Nachr.* **333**, 71-77 (2012)
- G.O. Roberts, Spatially periodic dynamos, *Phil. Trans. Roy. Soc. A* **266**, 535-558 (1970)
- G.O. Roberts, Dynamo action of fluid motions with two-dimensional periodicity, *Phil. Trans. Roy. Soc. A* **271**, 411-454 (1972)
- I. Rogachevskii, N. Kleeorin, Electromotive force and large-scale magnetic dynamo in a turbulent flow with a mean shear, *Phys. Rev.* **68**, 036301 (2003)
- I. Rogachevskii, N. Kleeorin, Nonlinear theory of a ‘shear-current’ effect and mean-field magnetic dynamos, *Phys. Rev.* **70**, 046310 (2004)
- I. Rogachevskii, N. Kleeorin, (, *Phys. Rev.* **76**, 056307 (2007)RK07) Magnetic fluctuations and formation of large-scale inhomogeneous magnetic structures in a turbulent convection
- A.S. Rubashny, D.D. Sokoloff, 58, *Moscow Univ. Phys. Bull.* **N2**, 5-87 (2010) Fully developed turbulent dynamo at low magnetic Prandtl numbers
- G. Rüdiger, Reynolds stresses and differential rotation I. On recent calculations of zonal fluxes in slowly rotating stars, *Geophys. Astrophys. Fluid Dynam.* **16**, 239-261 (1980)
- G. Rüdiger Differential rotation and stellar convection: Sun and solar-type stars. Gordon & Breach, New York (1989)
- G. Rüdiger, L.L. Kitchatinov, Do mean-field dynamos in nonrotating turbulent shear-flows exist?, *Astron. Nachr.* **327**, 298-303 (2006)
- A.A. Ruzmaikin, A.M. Shukurov, Spectrum of the galactic magnetic field, *Astrophys. Spa. Sci.* **82**, 397-407 (1982)
- A.A. Ruzmaikin, D.D. Sokoloff, A.M. Shukurov *Magnetic Fields of Galaxies*. Kluwer, Dordrecht (1988)
- A.A. Schekochihin, J.L. Maron, S.C. Cowley, J.C. McWilliams, The small-scale structure of magnetohydrodynamic turbulence with large magnetic Prandtl numbers, *Astrophys. J.* **576**, 806-813 (2002)
- A.A. Schekochihin, S.C. Cowley, J.L. Maron, J.C. McWilliams, Critical magnetic Prandtl number for small-scale dynamo, *Phys. Rev. Letters* **92**, 054502 (2004a)
- A.A. Schekochihin, S.C. Cowley, S.F. Taylor, J.L. Maron, J.C. McWilliams, Simulations of the small scale turbulent dynamo, *Astrophys. J.* **612**, 276-307 (2004b)
- A.A. Schekochihin, S.C. Cowley, R.M. Kulsrud, G.W. Hammett, P. Sharma, Plasma instabilities and magnetic field growth in clusters of galaxies, *Astrophys. J.* **629**, 139-142 (2005a)
- A.A. Schekochihin, N.E.L. Haugen, A. Brandenburg, S.C. Cowley, J.L. Maron, J.C. McWilliams, Onset of small scale dynamo at small magnetic Prandtl numbers, *Astrophys. J.* **625**, L115-L118 (2005b)
- A.A. Schekochihin, A.B. Iskakov, S.C. Cowley, J.C. McWilliams, M.R.E. Proctor, T.A. Yousef, Fluctuation dynamo and turbulent induction at low magnetic Prandtl numbers, *New J. Phys.* **9**, 300 (2007)
- D.S. Shapovalov, E.T. Vishniac, Simulations of Turbulent Dynamos Driven by the Magnetic Helicity Flux, *Astrophys. J.* **738**, 66 (2011)
- A. Shukurov, Introduction to galactic dynamos, in *Mathematical Aspects of Natural Dynamos*, EDP Press, eprint arXiv:astro-ph/0411739 (2004)
- A. Shukurov, D. Sokoloff, K. Subramanian, A. Brandenburg, Galactic dynamo and helicity losses through fountain flow, *Astron. Astrophys.* **448**, L33-L36 (2006)
- N.A. Silant’ev, Magnetic dynamo due to turbulent helicity fluctuations, *Astron. Astrophys.* **364**, 339-347 (2000)
- N.K. Singh, S. Sridhar, Transport coefficients for the shear dynamo problem at small Reynolds numbers, *Phys. Rev.* **83**, 056309 (2011)
- D.D. Sokolov, The disk dynamo with fluctuating spirality, *Astron. Rep.* **41**, 68-72 (1997)
- S. Sridhar, N.K. Singh, The shear dynamo problem for small magnetic Reynolds numbers, *J. Fluid Mech.* **664**, 265-285 (2010)
- S. Sridhar, K. Subramanian, Shear dynamo problem: Quasilinear kinematic theory, *Phys. Rev.* **79**, 045305R (2009)
- S. Sridhar, K. Subramanian, Nonperturbative quasilinear approach to the shear dynamo problem, *Phys. Rev.* **80**, 066315 (2009)
- K. Subramanian, Dynamics of fluctuating magnetic fields in turbulent dynamos incorporating ambipolar drifts, eprint arXiv:astro-ph/9708216 (1997).

- K. Subramanian, Unified treatment of small- and large-scale dynamos in helical turbulence, *Phys. Rev. Letters* **83**, 2957-2960 (1999)
- K. Subramanian, Magnetic helicity in galactic dynamos, *Bull. Astr. Soc. India* **30**, 715-721 (2002)
- K. Subramanian, L. Mestel, Galactic dynamos and density wave theory – II. An alternative treatment for strong non-axisymmetry, *Monthly Notices Roy. Astron. Soc.* **265**, 649-654 (1993)
- K. Subramanian, A. Brandenburg, Nonlinear current helicity fluxes in turbulent dynamos and alpha quenching, *Phys. Rev. Letters* **93**, 205001 (2004)
- K. Subramanian, A. Brandenburg, Magnetic helicity density and its flux in weakly inhomogeneous turbulence, *Astrophys. J.* **648**, L71-L74 (2006)
- K. Subramanian, A. Shukurov, N.E.L. Haugen, Evolving turbulence and magnetic fields in galaxy clusters, *Monthly Notices Roy. Astron. Soc.* **366**, 1437-1454 (2006)
- M. Steenbeck, F. Krause, Zur Dynamotheorie stellarer und planetarer Magnetfelder I. Berechnung sonnenähnlicher Wechselfeldgeneratoren, *Astron. Nachr.* **291**, 49-84 (1969) See also the translation in Roberts & Stix, *The turbulent dynamo*, Tech. Note 60, NCAR, Boulder, Colorado (1971).
- M. Steenbeck, F. Krause, K.-H. Rädler, Berechnung der mittleren Lorentz-Feldstärke $\overline{\mathbf{v} \times \mathbf{B}}$ für ein elektrisch leitendes Medium in turbulenter, durch Coriolis-Kräfte beeinflusster Bewegung, *Z. Naturforsch.* **21a**, 369-376 (1966) See also the translation in Roberts & Stix, *The turbulent dynamo*, Tech. Note 60, NCAR, Boulder, Colorado (1971).
- R. Stepanov, F. Plunian, Fully developed turbulent dynamo at low magnetic Prandtl numbers, *J. Turbul.* **7**, N39 (2006)
- S. Sur, A. Shukurov, K. Subramanian, Galactic dynamos supported by magnetic helicity fluxes, *Monthly Notices Roy. Astron. Soc.* **377**, 874-882 (2007)
- S. Sur, A. Brandenburg, K. Subramanian, Kinematic alpha effect in isotropic turbulence simulations, *Monthly Notices Roy. Astron. Soc.* **385**, L15-L19 (2008)
- S. Sur, K. Subramanian, Galactic dynamo action in presence of stochastic α and shear, *Monthly Notices Roy. Astron. Soc.* **392**, L6-L10 (2009)
- E.T. Vishniac, A. Brandenburg, An incoherent $\alpha - \Omega$ dynamo in accretion disks, *Astrophys. J.* **475**, 263-274 (1997)
- E.T. Vishniac, J. Cho, Magnetic helicity conservation and astrophysical dynamos, *Astrophys. J.* **550**, 752-760 (2001)
- J. Warnecke, A. Brandenburg, Surface appearance of dynamo-generated large-scale fields, *Astron. Astrophys.* **523**, A19 (2010)
- J. Warnecke, A. Brandenburg, D. Mitra, Dynamo-driven plasmoid ejections above a spherical surface, *Astron. Astrophys.* **534**, A11 (2011)
- T.A. Yousef, T. Heinemann, A.A. Schekochihin, N. Kleorin, et al., Generation of Magnetic Field by Combined Action of Turbulence and Shear, *Phys. Rev. Letters* **100**, 184501 (2008)
- T.A. Yousef, T. Heinemann, F. Rincon, A.A. Schekochihin, et al., Numerical experiments on dynamo action in sheared and rotating turbulence, *Astron. Nachr.* **329**, 737-749 (2008b)
- Ya.B. Zeldovich, Observations in a Universe Homogeneous in the Mean, *Astron. Zh.* **41**, 19-23 (1964) [*Sov. Astron.* **8**, 13-17 (1964)].
- Ya.B. Zeldovich, A. A. Ruzmaikin, D. D. Sokoloff *Magnetic fields in astrophysics*. Gordon and Breach, New York (1983)
- Ya.B. Zeldovich, A. A. Ruzmaikin, S. A. Molchanov, D. D. Sokoloff, Kinematic dynamo problem in a linear velocity field, *J. Fluid Mech.* **144**, 1-11 (1984)
- Ya.B. Zeldovich, A. A. Ruzmaikin, D. D. Sokoloff *The Almighty Chance*. World Scientific, Singapore (1990)